A framework for ground-up life cycle assessment of novel, carbonstoring building materials

Seth Kane ^{a, †}, Baishakhi Bose ^b, Thomas P. Hendrickson ^c, Jin Fan ^a, Sarah L. Nordahl ^c, Corinne D. Scown ^{b,c,d,e}, Sabbie A. Miller ^a

a Department of Civil and Environmental Engineering, University of California, Davis
 b Biological Systems and Engineering Division, Lawrence Berkeley National Laboratory
 c Energy Analysis and Environmental Impacts Division, Lawrence Berkeley National Laboratory
 d Joint BioEnergy Institute, Lawrence Berkeley National Lab
 c Energy & Biosciences Institute, University of California, Berkeley
 Corresponding Author: T +1 907 750 6364, E skane@ucdavis.edu

11 12 13

14

15

16

17

18

19

20

21

22

23

24

25

26

27

28

29

1

2

3

4

Abstract:

Currently, materials production of materials is responsible for over 25% of anthropogenic CO₂ emissions. However, due to their long-lived nature and enormous scale of production, some building materials offer a potential means for atmospheric carbon storage. Accurate emissions accounting is key to understanding this potential, yet life-cycle inventory (LCI) databases struggle to keep up with the wide array of novel materials and provide the data to accurately characterize their effect on net carbon dioxide equivalent (CO₂e) emissions and uptake. To this end, we offer a framework for developing LCIs from the ground up using thermodynamic first principles and provide guidance on alternative approaches to characterize material LCIs from limited data when first principles approaches are not feasible. This framework provides a generalizable methodology to develop and compare LCIs of novel material production. To ensure the accuracy of this framework and provide step-by-step examples of its application, we consider the following mineral-based and bio-based building materials: Portland cement, low-carbon steel, gypsum board, and cross-laminated timber from yellow poplar and from eastern hemlock, showing good agreement with existing LCIs. This framework is developed with a particular focus on describing CO₂e emissions and energy consumption of material production, but it could be extended to other environmental impacts or applications. Grounding initial LCIs in first principles can guide the early-stage design of novel materials and processes to minimize CO₂e emissions or improve the carbon sequestration potential of critical materials across sectors.

30 31 32

33

34

35

Keywords:

Carbon uptake; carbon sequestration; carbon dioxide removal; life-cycle inventory; industrial decarbonization

1. Introduction

Materials production accounts for approximately 25% of global anthropogenic greenhouse gas (GHG) emissions. ^{1,2} Building materials alone contribute nearly two-thirds of material emissions, and approximately 39 Gt of building materials were produced and used globally in 2019. ¹ Several groups, including the National Academies of Science, Engineering, and Medicine, have argued that building materials are particularly well suited to act as carbon dioxide removal (CDR) or carbon utilization systems due to their immense scale of production and long-lived applications, ³ and studies suggest up to 16.6 Gt of CO₂ could be stored in building materials annually. ⁴ However, to achieve carbon storage in building materials, rapid development and growth in novel materials for buildings and energy are required. ^{5,6} Accurate accounting of emission fluxes associated with the production of novel materials is needed to ensure carbon removal is achieved, and such data are challenging to accurately assess at early technology readiness levels. Therefore, to capitalize on material carbon storage potential, systemic accounting of material production emissions is needed early in the development process and with limited data availability.

To ensure that novel materials are low-emission or carbon-negative, their greenhouse gas (GHG) emissions must be quantified. However, life cycle assessments (LCA) of novel materials and processes are challenging due to inherent limitations in inventory data. To Due to the data-poor environment of novel materials production, life cycle inventory (LCI) data often must be extrapolated from similar processes or laboratory-scale experiments, leading to increased uncertainty in emissions and challenges in comparing the life cycle emissions of novel materials. A true apples-to-apples comparison of novel processes to an existing, commercial-scale operation is inappropriate when LCI data for novel processes only reflect laboratory or pilot-scale activities while high-quality, commercial data characterizes the existing technology. Furthermore, methods for estimating LCI data are often not standardized between studies, with past studies taking an individualized approach to the production processes they consider, which may not be applicable to accurately model other material production processes. Such differences make the comparison of results between studies that use different modeling methods and assumptions challenging.

Proposed methods to estimate LCIs when data are limited include proxy selection, development of machine learning models, chemical process simulation, or estimation based on the thermodynamic and chemical first principles of material synthesis. Past studies have shown that these methods have a fundamental tradeoff between data accuracy and data requirements, with specific-process data for a single facility being the most accurate but also requiring time-consuming and costly data collection, while proxy selection is the least accurate. 10 When new technologies are in the early stages of research and development (e.g., lab-scale), estimations based on first principles and thermodynamics may be the most accurate method for estimating LCI data using existing process data. Past studies utilizing first principles to estimate LCI data have varied in both the approaches taken to estimate such data and the process steps included in such analyses. When considering chemical conversion of raw resources into materials, past studies have all started with first principles to estimate energy requirement, such as enthalpy of reaction, and stoichiometric calculation of chemical-derived emissions, which have additionally been integrated into LCAs of current practice. However, these past methods have varied in how they address thermal efficiency, using estimations such as efficiency of similar commercial scale systems, ¹² constant assumed efficiency values, ^{10,13} or technology and fuel specific thermal efficiency values. 14 Mechanical processing has been based on existing commercial values, 12 process calculations, 10 or specifics of technology used.¹⁴ Further, transportation is assumed at a constant distance by all of these past studies, while all rely on existing LCI data for resource extraction.^{12,10,13,14} Such differences in approach and scope considered with these estimation methods drive differences in results for LCIs developed under data-poor conditions, creating a key gap in comparing LCA results for novel and data-poor materials production, which can impact decision making related to materials decarbonization.

Some process steps cannot be adequately modeled from first principles alone, including key resource extraction processes, such as mining and logging. Accurate modeling of these process steps when existing LCI data is insufficient is a key gap when comparing across past approaches to estimate LCI data from first principles. However, such data can be estimated with similar data requirements to first principles approaches by considering factors from the "ground up" based on process systems and design. For example, when examining forestry practices with limited data, considering species specific density and composition, herbicide application rates, terrain-specific forestry practices, and machinery energy use can allow for specific emission values to be used when known for a specific sub-process, and values can be estimated from the ground up based on typical practices for similar systems. The development of a systematic methodology that assesses LCIs of novel processes step-by-step, accounting for key material production processes using first-principles approaches integrated with a ground-up approach would improve the typically low accuracy of estimating LCIs at early development stages. Creating a standardized framework to determine such data could enable accurate comparisons between LCIs for novel materials, informing policy and development decisions surrounding industrial decarbonization.

To overcome data challenges with LCA, a ground-up, first-principles approach can simplify LCI data acquisition while focusing on the core processes in material production. A first-principles approach is considered a critical pathway to estimating LCI data. It could be well-suited for products reliant on chemical conversion for the production of key minerals or fossil-derived materials, such as cement, metals, or plastics. Such approaches have previously been applied to examine novel pathways for producing key chemicals while reconciling mass and energy balances, ¹⁵ to investigate alternative cement chemistries using a directly comparable methodological approach, ¹² and to compare different methods for estimating LCI data for key materials. 10 For some process steps, such as the growth and harvesting of biogenic resources or the mining of minerals, a first-principles thermodynamic approach would be extremely challenging to capture complex factors, including biomass growth and resource requirements. Therefore, first principles alone will not suffice in building a comprehensive LCI. In these cases, a firstprinciples approach for select process steps can be combined with a ground-up approach to assess flows based on equivalent process of each element of the product life cycle individually. Pairing this groundup approach with a first-principles approach when appropriate can help isolate data challenges in the life cycle to address and minimize uncertainties while maximizing accuracy for life-cycle stages where highquality data are available. A combined first-principles approach to model conversion processes and a ground-up approach to model other steps, such as resource extraction, could address data gaps in first principles-only LCI estimation methods. However, there is a need for a systematic methodological framework that can be broadly applied to materials production to create accurate and consistent LCIs for novel materials in data-limited environments.

 This work presents a systematic framework for assessing cradle-to-gate material environmental impacts with first principles approach to chemical conversion tied into assessment of other process steps based on equivalent flows to give a complete ground-up approach. While this framework could be applied to

- develop complete LCIs, we focus herein on GHG emissions and energy consumption, given the critical
- 2 role these impact categories play in CDR and decarbonization efforts. This framework is developed
- 3 step-by-step to provide necessary support in developing LCIs for novel, carbon-storing building
- 4 materials, given the urgent need for decarbonization and carbon storage in the built environment.
- 5 However, this framework is generalizable and can also be applied to materials in other critical sectors,
- 6 including, but not limited to, materials for renewable energy, battery materials, and biofuels. The
- 7 developed framework is applied to and validated for conventional building materials derived from both
- 8 mineral and biogenic resources, demonstrating the integration of ground-up and first-principles
- 9 components. This developed framework fills a critical need for a systematic method to determine the life
- 10 cycle inventories of novel materials and bridges the data accuracy gaps between first-principles
- 11 calculations and full process simulations.

14

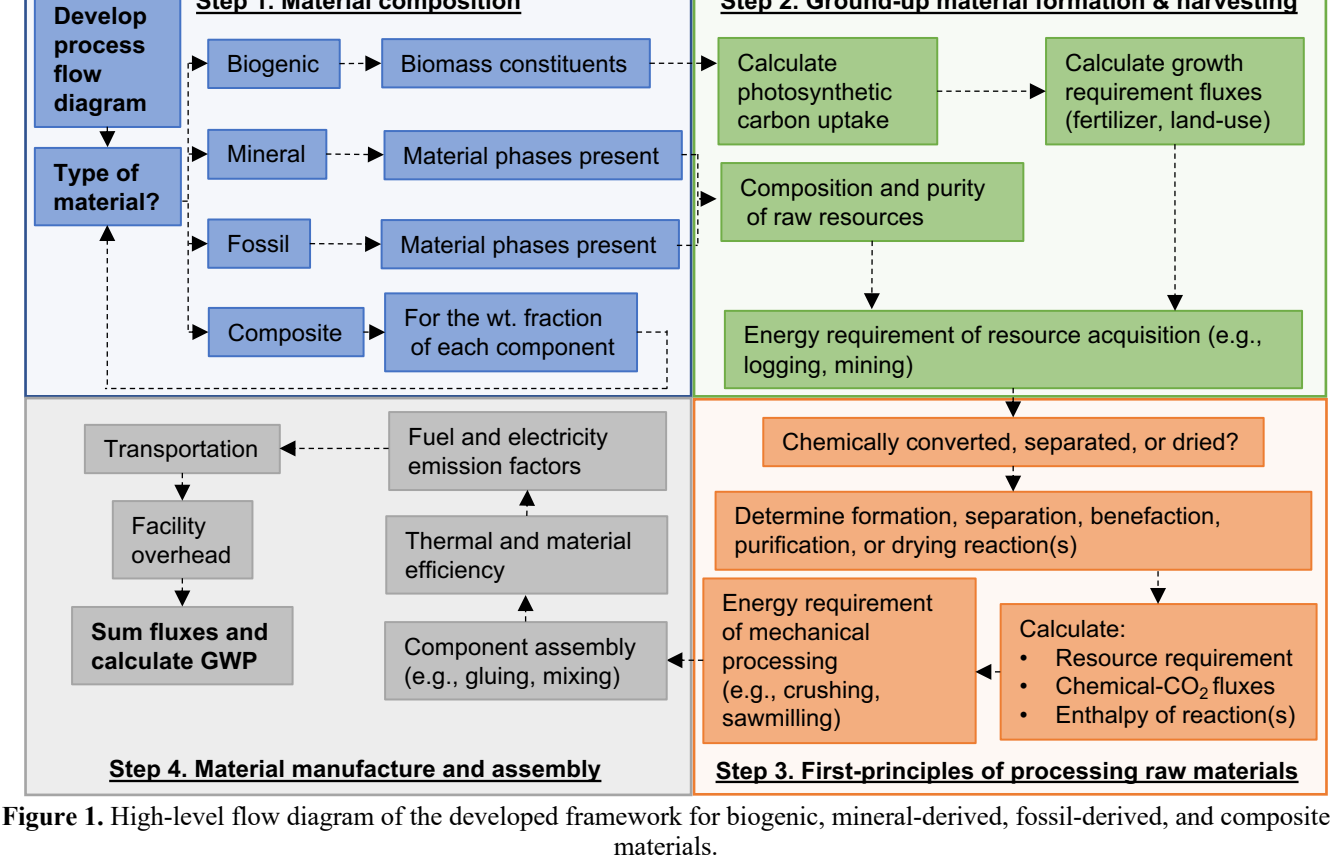
2. Methods

2.1 Analysis Framework

- 15 The developed framework (Figure 1) is broadly applicable to the production of materials and chemicals.
- In this framework, we pair a first-principles approach to estimating the LCI of chemical processing and
- 17 conversion with a ground-up approach to assess processes where estimating data from first principles
- would be challenging (e.g., biomass growth and harvesting, mining, or mechanical processing). By
- breaking down material production into individual process steps, this framework allows for the selection
- of higher-quality LCI data for any individual sub-process if available. The ground-up approach enables
- 21 the consideration of the role of individual process parameters on LCIs, based on existing data, to allow
- for a more robust estimation of these processes than proxy selection would provide.

23

- Herein, we focus on two primary material categories: biogenic and mineral-derived materials, given the
- critical role these material types play in the construction industry and their broad potential for carbon storage. The modeling approach taken for these material types primarily differs in the accounting of
- 27 material formation and harvesting (Sec. 2.1.2) processes, such as forestry and agricultural processes for
- biogenic materials and mining for mineral-derived materials. While chemical conversion processes are
- 26 biogenie materials and mining for mineral-derived materials. While chemical conversion processes are
- 29 more relevant for the production of mineral-derived materials, a similar approach could be taken for the
- 30 chemical processing of biomass. This framework could be adapted to other material classes (e.g., fossil-
- derived materials or chemicals, composite materials of multiple categories) by pairing a ground-up
- 32 approach to resource acquisition specific to the raw resources used with a first-principles approach to
- material processing and conversion. Composite materials can be considered a sum of their components,
- with component assembly considered in Step 4, and combined materials can be modeled either
- individually using the ground-up approach developed herein or by relying on existing LCIs. The
- 36 following subsections correspond to the steps of the framework shown in Figure 1.



Step 2. Ground-up material formation & harvesting

2.1.1 Material Composition

1 2 3

4 5

6

7

8

9

10

11 12

13 14

15 16

17 18

19

20

21

22

23

24 25

26

27

Detailed knowledge of material phase composition is crucial for determining the formation reactions of material phases and raw resource requirements prior to any formation reactions. For biogenic materials, this includes the composition of constituent biomass phases (e.g., cellulose, lignin, moisture, and carbon content) to inform modeling inputs and outputs throughout the material life cycle. For example, as tabulated in Supplemental Tables 1 and 2, specific biomass species will have composition variations depending on growing methods and regions, which impact carbon fluxes, processing requirements. performance in use, and final potential for reuse and recovery. Additionally, at this stage, a process flow diagram for material production (e.g., Figure 2 or 3, Supplemental Figures 1 or 2) should be created to aid in determining process parameters for future steps, and a system boundary should be defined.

2.1.2 Raw material formation and harvesting

Step 1. Material composition

A ground-up approach is taken to material acquisition processes, such as biomass growth and mineral mining. First, the composition of the raw material is determined, such as mineral phases present (e.g., calcite, silica, hematite in common mineral resources) or biogenic constituents (e.g., cellulose, hemicellulose, lignin, ash, and moisture content). This analysis can rely on previously reported literature values as is done herein for mineral resources (see Section 2.3), or similar approaches can be used with site-specific mineralogy information, biogenic resource composition, or composition of fossil feedstocks.

For biogenic materials, growth and harvesting resources will vary by species, material composition, and growing region. Differences in determining carbon stored in growth will meaningfully affect overall life-cycle impacts. Carbon fluxes in plant growth can be highly uncertain and sensitive to various

factors, including local climate, soil conditions and composition, nutrient availability, genetic variation in individual tree populations, and other environmental influences. 19,20 Identifying accurate estimates for carbon storage can be challenging. For our framework application (see Section 2.3), we utilized existing literature specific to a specific region and lumber species. Other biogenic carbon literature and databases, such as the recent Roads to Removal report which studied pine forest carbon stocks, 19 can be helpful in generating carbon storage estimates. For cultivated biomass that requires fertilizer application, nitrogen inputs are a key driver of GHG emissions, both due to the energy-intensive production and because several percent of applied nitrogen is subsequently emitted as N₂O. What is common practice in LCA, and can be used as a simplified approach, is sourcing compositional data for specific biomass types and assuming that, for managed agricultural lands, supplemental nitrogen must be added in an amount equivalent to the nitrogen contained in any removed biomass (e.g., 1 kg of N in fertilizer added for each kg of N contained in biomass that is removed from the field). The approach does not require a specific model but requires accurate compositional data for the biomass that is removed. This approach is conservative, as leaving excess biomass with a high C:N ratio can have nitrogen immobilization effects and compete with the crop for fertilizer, requiring additional nitrogen fertilizer to be added beyond what would otherwise be required by the crop. However, the degree to which this happens is dependent on soil conditions and how the crop is managed on a multi-year basis.²¹ Additionally, for biogenic materials, other inputs and resource requirements for crop cultivation and harvest need to be considered in capturing life-cycle impacts; however, they do not typically incorporate a first principles approach, as we expect LCI data to be readily available. These data include material inputs such as herbicides, insecticides, and fuel use in harvest equipment, which should be obtained from relevant models (e.g., the GHGs, Regulated Emissions, and Energy use in Technologies [GREET] model²²), existing LCI data, and literature for specific biomass species and locations. In this study, the growth and harvest stage of the framework for biogenic materials was developed based on previous literature and LCI datasets. 22-25

Notably, biomass cultivation also involves carbon uptake during biomass growth. To calculate the CO₂ equivalent stored in the final product (e.g., CLT), a carbon content of 50% of the total wood was used; although, specific carbon contents of individual biomass resources may be substituted. Based on stoichiometric balance calculations, we modeled CO₂ uptake as 3.67 times the carbon content. Cradle-to-gate GHG emissions presented in subsequent discussions are shown, both excluding and including biogenic CO₂ uptake and emissions, to perform a harmonized validation comparison with past studies.

For logging and other agricultural harvesting processes, refinement of the LCI based on location is critical, as logging operations differ depending on the type(s) of forest and local topography, including slope. These factors not only impact energy demand for logging and transportation but also the expected biomass availability each year, tied to sustainable removal rates.

Robust LCIs exist for current mining resources and extraction methods, which can be leveraged for processes that utilize existing mineral resources in novel materials or processes. In these cases, emissions from mining can be evaluated using existing LCI data (e.g., from ecoinvent²⁶ or the US LCI database²⁷) associated with the mining, quarrying, and extraction of these resources. However, even for well-established mineral extraction methods, there is meaningful spatial variation in the purity, extraction depth, mining method used, and other factors, which is expected to result in variations in emissions associated with mining and fossil extraction processes. For novel mineral extraction processes, emissions should be estimated using a ground-up approach based on data for similar extraction methods, depth, hardness, and mineral composition.

2.1.3 Processing and conversion of raw materials

The analysis of material formation and procurement differs for materials that are chemically converted or separated during processing compared to those that are not. For materials that undergo chemical transformation or separation (e.g., common mineral-derived materials or biorefineries), the initial step of this stage is determining the chemical reactions required to form the final material from raw material resources. Based on the formation reactions, the following are determined:

- 1. The stoichiometrically required raw material phases are determined from the chemical reaction based on the molar ratios of feedstocks to products and the relative molecular weights. Based on these values and the raw material composition determined in Step 1, the mass of raw mineral resources required can be determined.
- 2. GHG fluxes, most commonly CO₂, into or out of mineral resources can be determined based on the stoichiometry of the reaction and are referred to as chemically derived emissions. For example, in the reaction to form lime from limestone (CaCO₃ → CaO + CO₂), one mol of CO₂ is released per mol of lime formed or 0.79 kg CO₂ / kg lime.
- 3. The thermodynamic energy requirement of the reaction can be determined based on the standard enthalpy of the reaction, calculated as the sum of the standard enthalpy of formation of the products minus the sum of the standard enthalpy of formation of the reactants, with the equation:

 $\Delta H_{Rxn,x} = \frac{\sum_{products} n_p \cdot \Delta H_{f,p}^o - \sum_{reactants} n_r \cdot \Delta H_{f,r}^o}{n_x}$ (1) In this equation, $\Delta H_{Rxn,x}$ is the enthalpy of reaction per mol of product, x, $\Delta H_{f,p}^o$ is the standard

In this equation, $\Delta H_{Rxn,x}$ is the enthalpy of reaction per mol of product, x, $\Delta H_{f,p}^{o}$ is the standard enthalpy of formation of each product, and n_p is the number of mols of each product, and similarly for each reactant, r.

We note that values of chemical CO₂ emissions and enthalpy of reaction for mineral-derived materials using production methods typically used in the United States have previously been tabulated.²⁸ These tabulated values may provide additional guidance on determining these critical inputs for novel materials.

Separation, benefaction, and purification processes are often performed after mineral extraction, in biorefineries to separate biogenic constituents, or in the processing of fossil resources to eliminate impurities and separate co-products. Typically, these processes do not convert the chemical structure of the material extracted material but may lead to chemical reactions of other mineral material phases present, other reactants, or the formation of intermediate products. Therefore, a similar first-principles method can be applied to estimate LCI data as was done for chemical conversion. Such analysis has been reported in detail in a past study examining utilizing first principles to determine LCIs of chemical production. We note that GHG emissions associated with secondary inputs required for chemical reactions can be estimated via first principles or ground-up approaches as described above, or a past LCI or proxy can be utilized. In industrial production, separation processes are often highly synergistic, yielding multiple products. Allocation of emissions to co-products can be performed or avoided using methods similar to those employed in conventional LCA.

For many biogenic materials, drying of moisture content is a key process step prior to other processing. For example, green logs may enter a mill at 50% moisture content and be dried to 10%. The enthalpy of vaporization for water dictates minimum drying energy (40.7 kJ/mol or 2.3 MJ/kg of water).

To model mechanical processing, we implement a suite of strategies. For processing such as crushing, grinding, and milling processes, we implement Bond's equation²⁹, which relates the energy used during a size-reduction process (W) to the starting particle size (80% passing particle size, F), ending particle size (80% passing particle size, P), and the Bond index, an experimentally-derived constant specific to a particular mineral (W_i) :

(2)

 $W = \frac{10 \cdot W_i}{\sqrt{P}} - \frac{10 \cdot W_i}{\sqrt{F}}$ The Bond index has been reported for a wide variety of minerals by Bond²⁹ and has since been further refined by additional studies. Energy use during mechanical processing was calculated with this equation with P and F values typical for the input minerals post-mining and final material product. Methods such as this, which directly relate energy inputs to the processing conditions of the resources and products, can be utilized to inform LCIs for other grinding processes. For other mechanical processing, such as sawmilling of wood, a ground-up approach is taken, utilizing data on mechanical processing assembled from wood processing facilities, including sawmills and CLT mills. Based on the type of product(s) and wood type (hardwood vs. softwood), a ground-up decision tree approach was developed for sawmilling (Figure 9) using existing literature. ^{30–33}

2.1.4 Manufacturing and material assembly

1

2

3

4

5

6

7

8 9

10

11 12

13

14

15

16

17 18

19

20

21

22

23

24

25

26

27

28 29

30

31 32

33 34

35

36

37

38

39

40 41

42 43

44

45

46 47

The first principles-based approach will inform direct enthalpy requirements for chemical conversion. However, the inherent inefficiency of equipment must also be addressed to determine energy demand and associated GHG emissions from energy resource use. Enthalpy requirements apply only to materials that undergo chemical conversion, but energy inefficiencies apply broadly to material production. For processes that use standard conversion technologies (e.g., blast furnaces, rotary kilns, final lumber processing), process energy efficiency can be estimated by considering the efficiency of similar facilities, considering both methods of conversion, process length, and process temperature. Data are widely available for standard processes through numerous sources, such as the Manufacturing and Energy Conversion Survey (MECS), which is used herein. 33,34

For biomass drying, past estimates for total energy use range from 2.8 to 6 MJ/kg water, indicating that the enthalpy of vaporization (2.3 MJ/kg water) provides a useful minimum, and drying efficiency may vary from approximately 40-80% depending on technology. 35 Drying processes often combust residues (biomass) to provide this energy, but in some cases, another energy source is imported.

The energy grid and fuel mixtures used to generate energy for all material production and conversion processes, along with their associated emission factors, can be estimated via methods similar to conventional LCA, such as by using emission factors reported by the US Environmental Protection Agency.³⁶ These emission factors can be applied to energy requirements determined in earlier steps based on energy type (e.g., electric or thermal) and can then be modified to examine the sensitivity of results to specific energy resources; see Supplemental Table 5 for the emission factors used herein.

Beyond energy efficiency, material losses due to dust and spillage for mineral materials, as well as yield efficiencies for biogenic materials, should be considered for all steps of the production process. We note that material losses during chemical processing do not include chemically derived emissions, such as CO₂ released from chemical reactions, which are accounted for separately. The impact of material losses on total GHG emissions and energy requirements varies depending on the point of the losses during the production process, so losses should be accounted for individually at each processing stage. If multiple materials are combined into a full product (e.g., mixing of clinker and gypsum to form Portland cement

or resin and wood in CLT), material input LCIs should be combined at this step. The manufacturing step of the decision tree framework for this study was developed using dataset from existing literature. 17,37

Transportation should be modeled as in conventional LCAs, based on established truck, rail, and boat emission factors in kg CO₂e/kg·km.^{27,38} We note that transportation distances are highly site-specific and may not be accurately estimated from lab or pilot-scale data. As with process efficiency, facility overhead, including facility HVAC, lighting, onsite transportation, and other facility energy consumption not directly associated with the production of materials, can be informed by existing analyses of comparable facilities (e.g., MECS for US-wide overhead values for common materials³⁴).

2.2 Framework validation for mineral-derived materials

To validate the developed framework, it is applied to several common mineral-based building materials, namely Portland cement, low-carbon steel, and gypsum board. For presentation purposes, we focus our discussion on Portland cement, which has global use, a variety of resource inputs, and a broad availability of existing LCI data for comparison. Portland cement is examined with production processes and mineral feedstocks that are typical of primary production in the United States, with a cradle-to-gate scope and a functional unit of 1 kg of final material (Figure 2). For all data inputs, data from 2019 or the closest available year prior to 2020 is used. To validate the framework, we model the LCI of Portland cement as if quality LCI data did not exist. However, to obtain equivalent data that would be available for novel processes, we draw on existing process data that is representative of the US average production. The details of the analysis for low-carbon steel and gypsum board are presented in the Supplemental Information, where we demonstrate the application of the framework to more complex thermal processing during steel production and to composite materials and drying during gypsum board production.

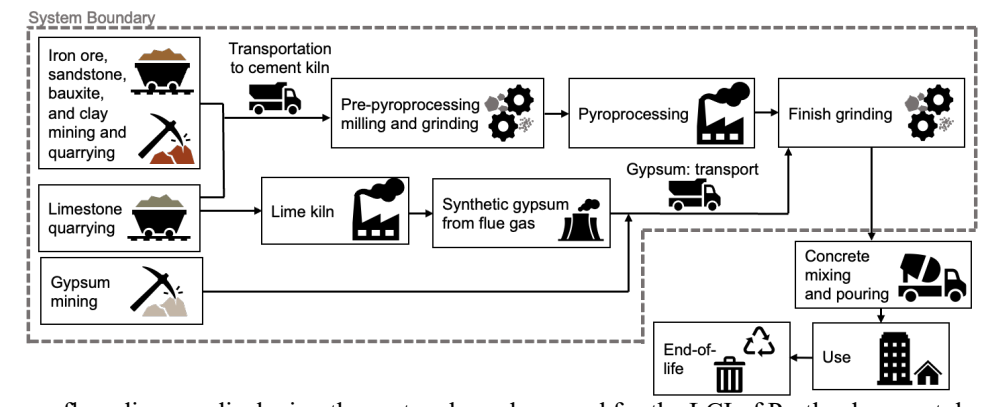


Figure 2. Process flow diagram displaying the system boundary used for the LCI of Portland cement described herein.

Portland cement typically contains the mineral phases alite (Ca₃SiO₅), belite (Ca₂SiO₄), ferrite (Ca₄Al₂Fe₂O₁₀), and aluminate (Ca₃Al₂O₆), with gypsum (Ca₂SO₄·2H₂O) added during finish grinding to control setting rate. The ratio of these mineral phases may vary depending on the type of Portland cement and processing facility but herein is modeled with ratios typical of Type I Portland cement (63% alite, 15% belite, 9% ferrite, 8% aluminate, 5% gypsum¹²) which comprises ~75% of US cement production,³⁹ abbreviated herein as "cement."

Mineral phase inputs are determined from chemical reactions of cement formation (Supplemental Table 3), and the mineral inputs for these phases are from the USGS Mineral Yearbook (2019)³⁹ data and analyses of this data²⁸ for cement, excluding waste or byproduct resource inputs. Material losses due to

dust, spillage, and other sources were considered; however, literature values for material losses during these steps vary greatly by study. ^{40–42} Furthermore, the impact of this variation on total GHG emissions and energy requirements varies depending on the point at which the losses occur during the production process, with fewer emissions embodied in losses prior to pyroprocessing. The NSF International Product Category Rule (PCR) for cement specifies a 5% estimate for material loss during production if other data is unavailable. ⁴³ Past LCA studies report varying total material losses across the entire cradle-to-gate production process, typically 7-11 wt.%. ^{40–42,44} Due to the meaningful variations in data for individual steps and to match the reported values for total material losses, a 3% loss value was used for all steps after mining, except for storage, which was modeled at 1%, resulting in a total material loss of 10.4% across all process steps.

Cement pyroprocessing is modeled as a single step, including preheating, pre-calcining, and the rotary kiln. Enthalpy of formation, resource requirements, and chemically derived emissions from pyroprocessing are assessed for each mineral phase individually and associated emissions are then combined (Supplemental Table 3). No separation processes were modeled for cement, as these processes are not typically used for this product. The mineralogy of raw mineral resources is determined from the literature. 45–50 However, we note that for some mineral resources, this is an area of significant spatial variation. LCIs for the mining and quarrying process of these materials are determined using ecoinvent with US data. Crushing and milling processes were modeled using Bond index values and particle sizes, as shown in the Supplemental Information, with electricity serving as the energy source. An energy efficiency value of 54.5% was used, as determined from MECS, by dividing the required energy reported by total energy inputs. An average US electricity grid and the average US fuel mix for cement production were used as electricity and fuel emission factors. 51

Transportation is excluded from our mineral material case studies due to its high variability.⁵² Transportation distances between the mine or quarry and the cement production facility are often considered negligible,⁵¹ as facilities are located at limestone quarries, and relatively small amounts of other minerals are used. However, the potential future implementation of transportation distances is included in the developed framework.

2.3 Framework validation for biogenic materials

For biogenic materials that undergo limited chemical processing, a limited first-principles approach can be combined with a ground-up decision-tree approach to assemble likely supply chains and individual processes required, making the assembly of the LCI more tractable. We address these assessment challenges by applying the framework to a case study of cross-laminated timber (CLT) products from yellow poplar (YP) and eastern hemlock (EH). The scope for YP CLT is shown in Figure 3 and details for EH CLT are provided in the Supplemental Information.

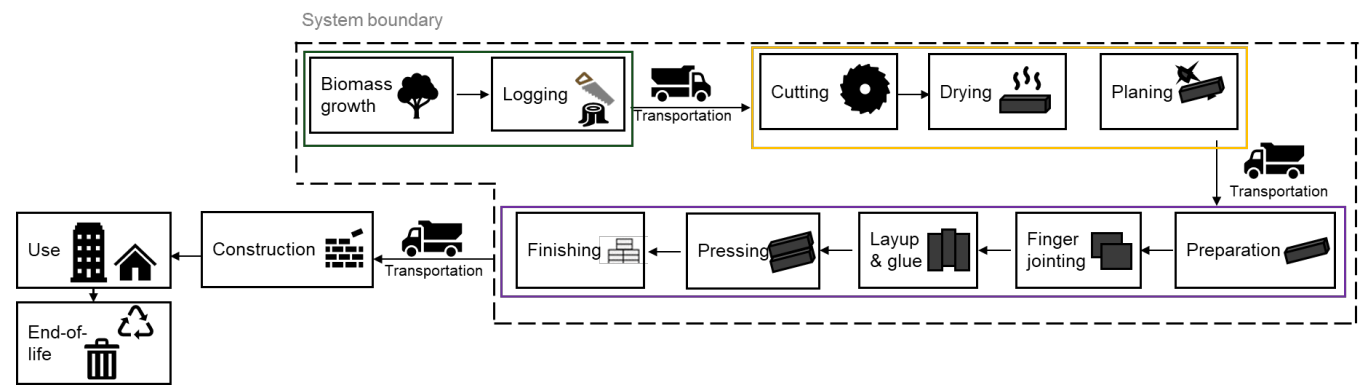


Figure 3. Process flow diagram displaying the system boundary used for the LCI of YP CLT described herein. The green, yellow, and purple rectangle shows the harvest, sawmilling, and CLT mill processes, respectively.

The validation study conducted herein on YP CLT is based in Tennessee, USA, as YP is abundant in the area, and sawmills in Tennessee already possess the equipment and knowledge necessary to process YP logs for CLT manufacturing. CLT-specific considerations for a cradle-to-gate LCI include forestry operations through the manufacturing of the CLT, as highlighted in Figure 3. To model inputs to CLT production, we have utilized a physical units-based input-output life-cycle inventory model, Agile-Cradle-to-Grave (Agile-C2G), which has been previously documented in the literature. ^{53–58} In this study, a functional unit of 1 m³ of CLT was used for ease of comparison with previously published literature on LCA of CLT. Life cycle inventory inputs and emission factors for each input parameter are provided in Supplemental Tables 5 and 6, respectively, based on previously published literature and LCA databases ^{17,22,26,27,59–62} and communications with local sawmills, with inputs adjusted where necessary to represent YP production. The assessment includes product transportation by truck between the harvest and the sawmill (50 km), and the sawmill to the final CLT production (61.2 km).

For the GHG fluxes associated with wood harvest and transport operations, a ground-up approach is employed based on the cradle-to-gate inputs and outputs from previously published literature^{23,25} and LCI databases, incorporating material inputs specific to the harvesting stage of growth. Based on previous literature,³⁰ our study assumes harvesting operations included the application of herbicides each year during the growing period, and the trees were harvested after 21 years. For logging operations, it was assumed that a shelterwood cutting method would be implemented using a feller-buncher-based harvesting system, and energy for logging was modeled based on previous literature.^{25,30,31}

Using biogenic material properties and the final properties of the product, mass flows through each process step can be estimated. Kiln-dried and sawn lumber is the wood input for the final processed biogenic material considered in this study (i.e. CLT). The output from the sawmill is finished logs. The sawmill processing steps include all debarking, sawing, chipping, and grinding required to convert logs into rough, dry lumber. The wood waste generated during the process is used in generating energy onsite, with upstream emissions allocated on a mass basis. For this analysis, we considered fossil CO₂, CH₄, and N₂O emissions and excluded biogenic CO₂ emissions. As with other processes, the sawmill's operational energy demand cannot be directly linked to the biogenic resource characteristics, so data related to processes involved in the sawmill were adapted from data from the Southeast regions by Milota and Puettmann.⁶⁵ The weighted average amount of wood in a CLT panel is 427 kg/m³. To produce this amount, a total of 517 kg (1.21 m³) of oven-dry lumber is required.^{17,63} This dry wood would, in turn, need 869 kg of green wood. Of this, 83% is assumed to be utilized to produce CLT, while the rest is assumed to be co-product (sawdust, chips, shavings, etc.). ^{17,63}

1 3. Results

- 2 3 A decision tree for the developed framework is shown in Figure 4, with details of the developed ground-
- up analysis for forestry and logging provided in Figure 9. Validation examples of the application of this
- 4 framework are given below for key materials.

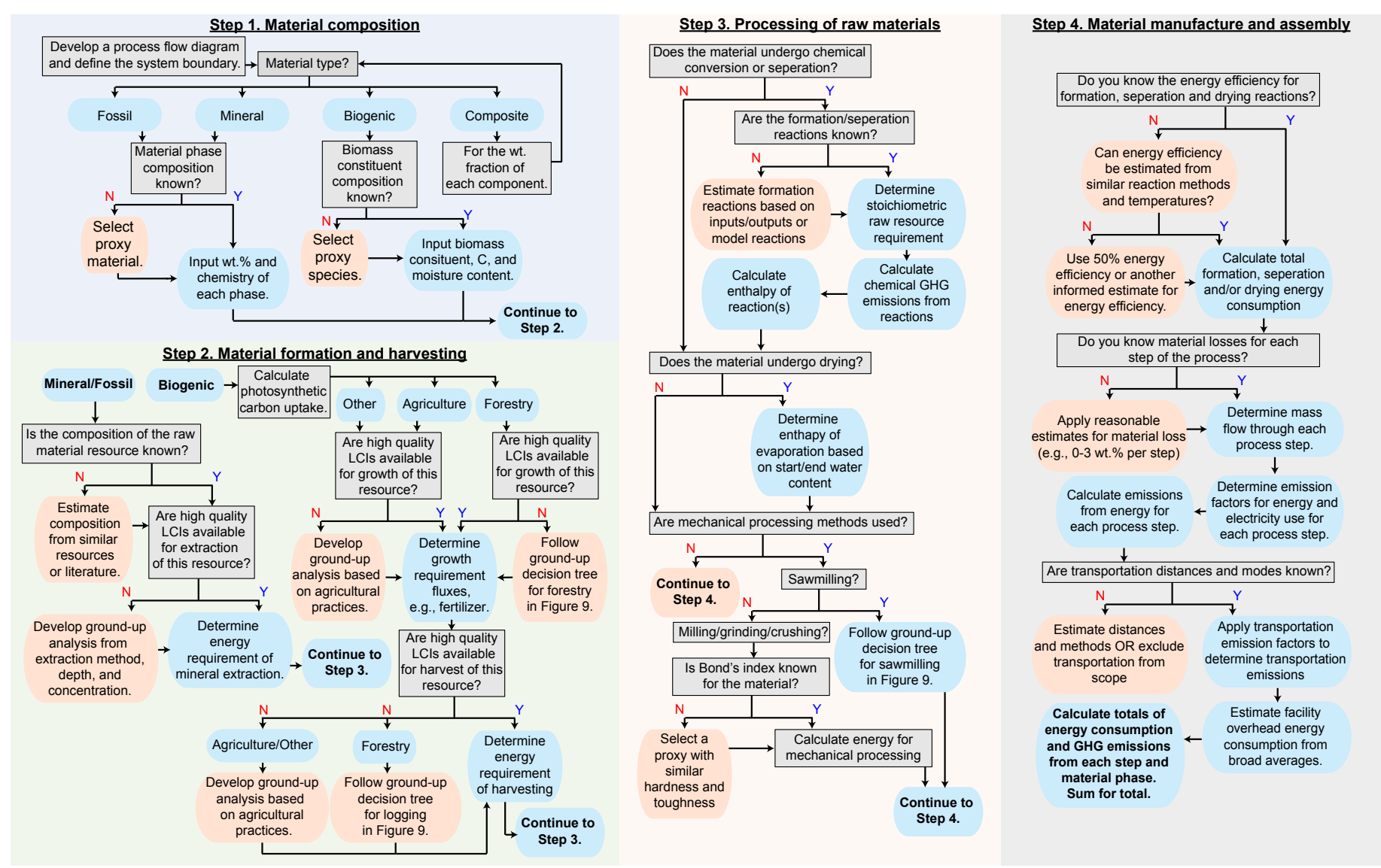


Figure 4. Decision tree of the developed ground-up framework for determining an LCI of a material.

1 2

3.1 Complete assessment and validation of Portland cement

3.1.2 Material formation and harvesting

From the formation reactions of manufacturing cement, mineral phase requirements were stoichiometrically determined and are shown in Figure 5a. As a result of impurities, mass loss due to material waste, and chemically-derived emissions, a total mass of 1.97 kg mineral is extracted / kg Portland cement, with the distribution of minerals shown in Figure 5d. Extraction of these resources requires an energy consumption of 0.165 MJ / kg Portland cement.

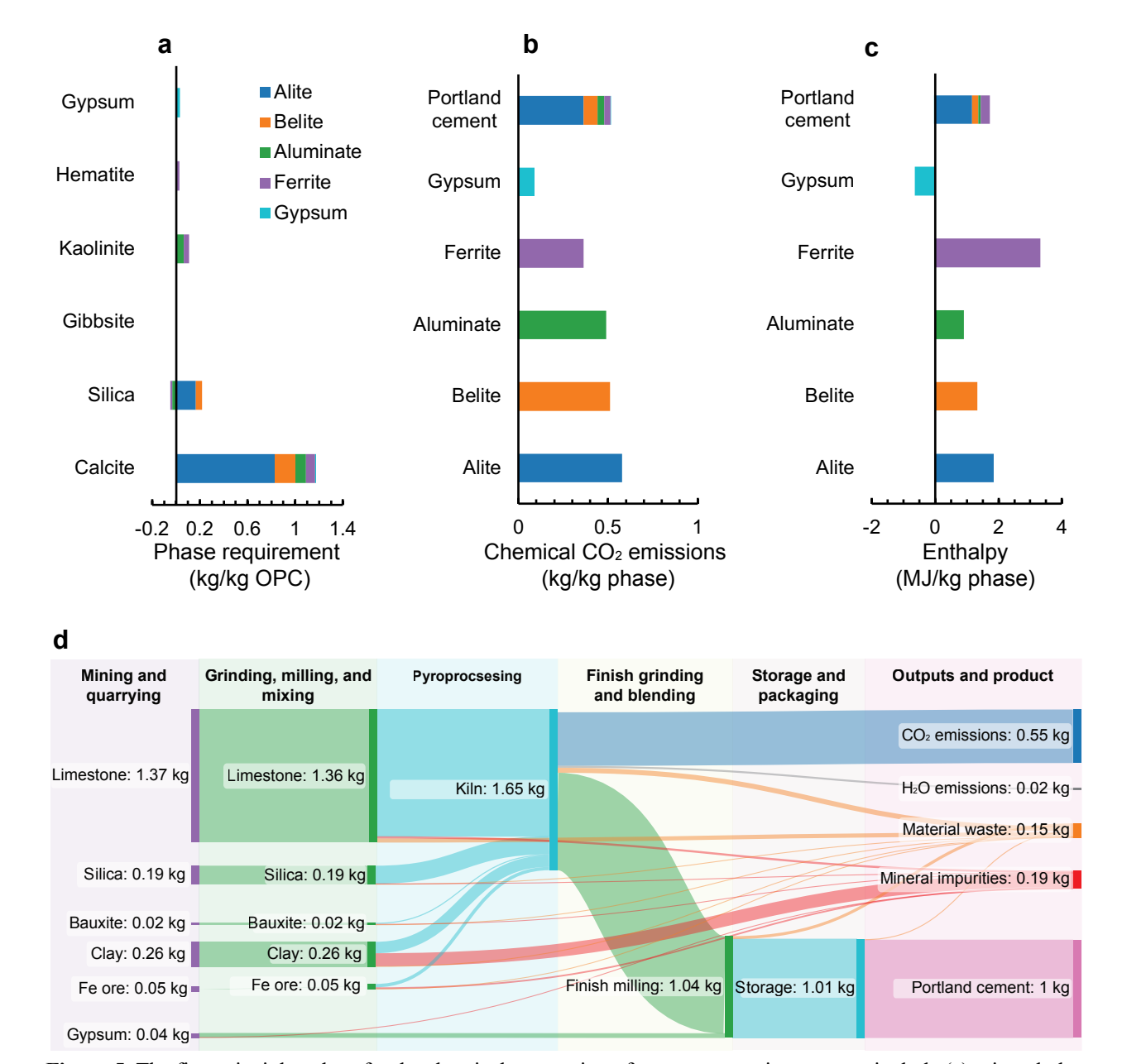


Figure 5. The first principle values for the chemical conversion of raw resources into cement include (a) mineral phase requirement, (b) chemically derived CO₂ emissions, and (c) energy required by the enthalpy of the reaction. Results in (b) and (c) are displayed for 1 kg of each cement phase and the total of 1 kg of Portland cement. (d) Sankey diagram of mass flows through the Portland cement production process showing raw resource requirements, material losses, material purity, and chemical emission values used in the first-principles LCI. We note that in some cases, material impurities may instead be double counting of consumed material that was not considered herein (e.g., silica in clay).

3.1.3 Processing of raw materials

Chemically-derived CO₂ emissions resulting from different Portland cement production pathways are weighted based on the mass ratios of each method (Supplemental Table 3, Figure 5b), resulting in chemically derived emissions of 0.548 kg CO₂ / kg Portland cement. The enthalpy of reaction for the production of Portland cement is 1.70 MJ / kg Portland cement, with a majority of the contribution being due to the alite phase (1.16 MJ / kg Portland cement, Figure 5c). Production reactions for aluminate from bauxite and synthetic gypsum from calcite are exothermic. For the production of aluminate from bauxite, this reaction would occur simultaneously with other endothermic reactions during cement making and, therefore, is credited against their energy requirements. In contrast, synthetic gypsum production is performed as an independent process, and its energy is not typically recaptured; therefore, it is not included in the energy total.

Grinding and milling processes prior to pyroprocessing result in an energy consumption of $0.215 \, \text{MJ} / \text{kg}$ Portland cement, primarily due to limestone (0.153 MJ / kg), while post-pyroprocessing milling and grinding result in an energy consumption of $0.118 \, \text{MJ} / \text{kg}$.

3.1.4 Material manufacture and assembly

The modeled pyroprocessing efficiency of 54.5% results in a 1.76 MJ / kg cement increase in the energy consumption over the enthalpy. Further, with the modeled rates of material waste, 0.146 kg of additional material is processed through at least one step, with an increase in mass flow through the high emission and energy requirement pyroprocessing step of 7.15%. Facility overhead values, inclusive of HVAC, onsite transportation, and facility lighting, result in energy consumption of 0.04 MJ / kg cement. We note that due to the limited number of significant figures present in the MECS data, this is an area of significant uncertainty and likely an area where there are large variations between cement production facilities. As such we examine this factor with sensitivity analysis (Sec. 3.5).

3.1.5 Portland cement total energy and GHG emissions validation

In total, the energy consumption of cement production is dominated by the pyroprocessing process, with 85% of the total energy consumption resulting from pyroprocessing and 42% of the total energy consumption required by the pyroprocessing enthalpy of reaction (Figure 6). Similarly, GHG emissions from the production of cement are dominated by pyroprocessing, with 59% of total GHG emissions resulting from chemically derived emissions during pyroprocessing.

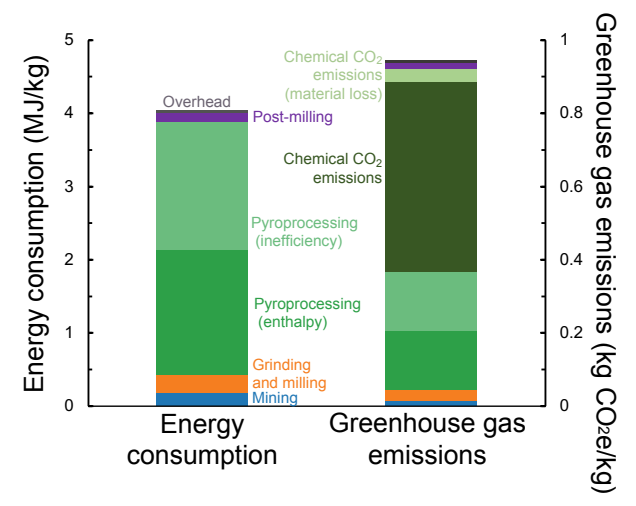


Figure 6. Totaled results for energy and GHG emissions for Portland cement, showing the contribution of each process step.

The GHG emissions determined with the ground-up approach (0.94 kg/kg cement) are in good agreement with the value determined by the PCA EPD (0.92 kg/kg Portland cement).⁶⁴ Similarly, good agreement is seen in the chemical emissions resulting from pyroprocessing (this study: 0.548 kg CO₂-eq / kg, PCA: 0.480 kg CO₂-eq / kg Portland Cement) and energy consumption (this study: 4.04 MJ / kg, PCA: 3.88 MJ / kg). The small differences between these analyses are driven by a difference in clinker content of 95% in our model versus 91.4% in the PCA EPD. When normalizing by clinker content, both the ground-up LCI and the PCA EPD show energy consumption of 4.25 MJ / kg clinker.

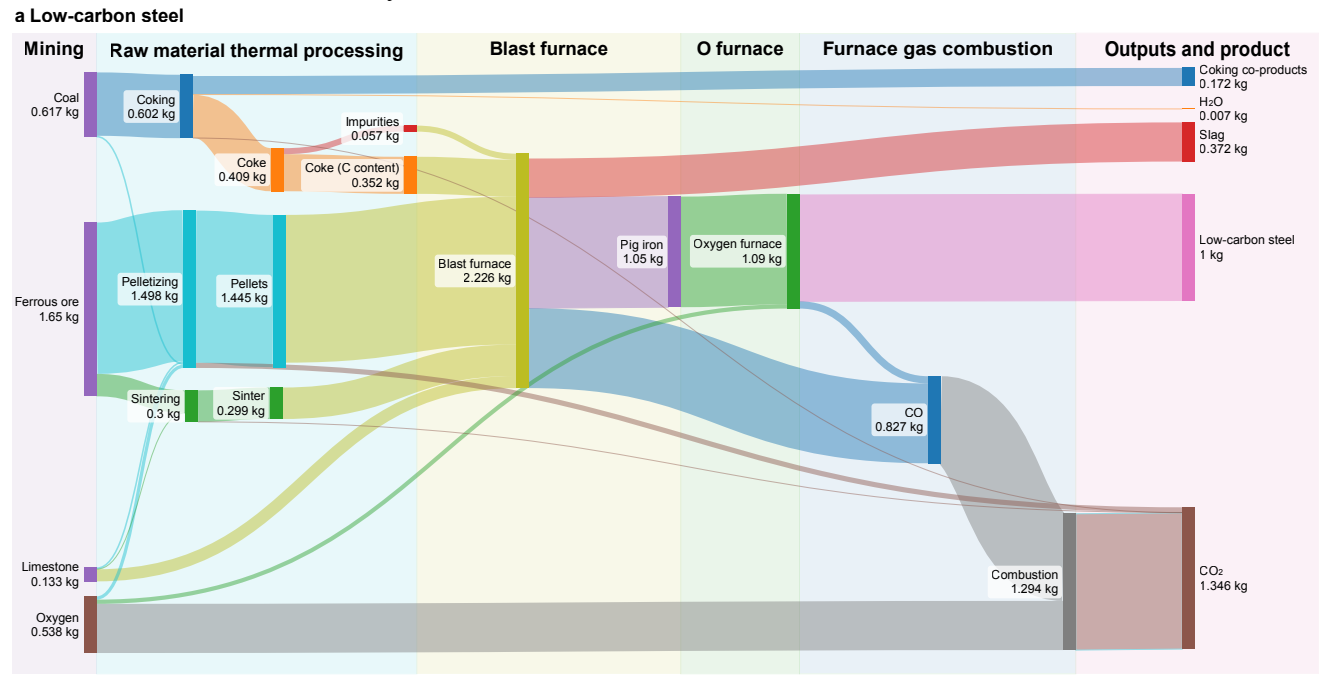
The GHG emissions determined herein also agree with other broad analyses of the cement industry. For example, the Cement Sustainability Initiative, in an analysis of 618 cement production facilities globally, reports average GHG emissions of 0.842 ± 0.101 kg CO₂e / kg Portland cement. These emissions are again comparable to the values determined herein (within one standard deviation for GHG emissions and within 3% for energy consumption). As global production is expected to have lower clinker content than US production, the lower emissions are again primarily due to this factor. Similarly, the US LCI entry for Portland cement ("Portland cement, at plant, US" ²⁷) reports GHG emissions of 0.927 kg CO₂e / kg Portland cement, 1.7% lower than the value determined herein, and energy consumption of 5.47 MJ / kg Portland cement.

3.2 Challenges presented by other common mineral-derived materials

In addition to cement, the developed framework was validated for low-carbon steel and regular-type gypsum board (See Supplemental Information for full methods and results). Mass flow diagrams of steelmaking and gypsum board production are shown in Figure 7, and process flow diagrams are shown in Supplemental Figures 1 and 2.

Steelmaking results in slag, coking gas, and blast furnace gas co-products. In the primary analysis, no emissions are allocated to the slag co-product. In comparison with Worldsteel⁶⁶ and International Energy Agency (IEA)⁶⁷ steel emission values, we apply a system expansion approach to account for slag replacement of primary cement production, using the emissions and energy for cement production from the analysis performed herein. No allocation is performed to coking co-products – all emissions associated with potential downstream processing or use of these products are excluded. We examine three allocation scenarios for CO₂ emissions associated with the oxidation of carbon monoxide produced by the reduction of iron ore to the energy co-product: (1) all oxidation emissions allocated to low-carbon

steel, (2) system expansion to include equivalent primary electricity production, and (3) all oxidation emissions allocated to electricity.



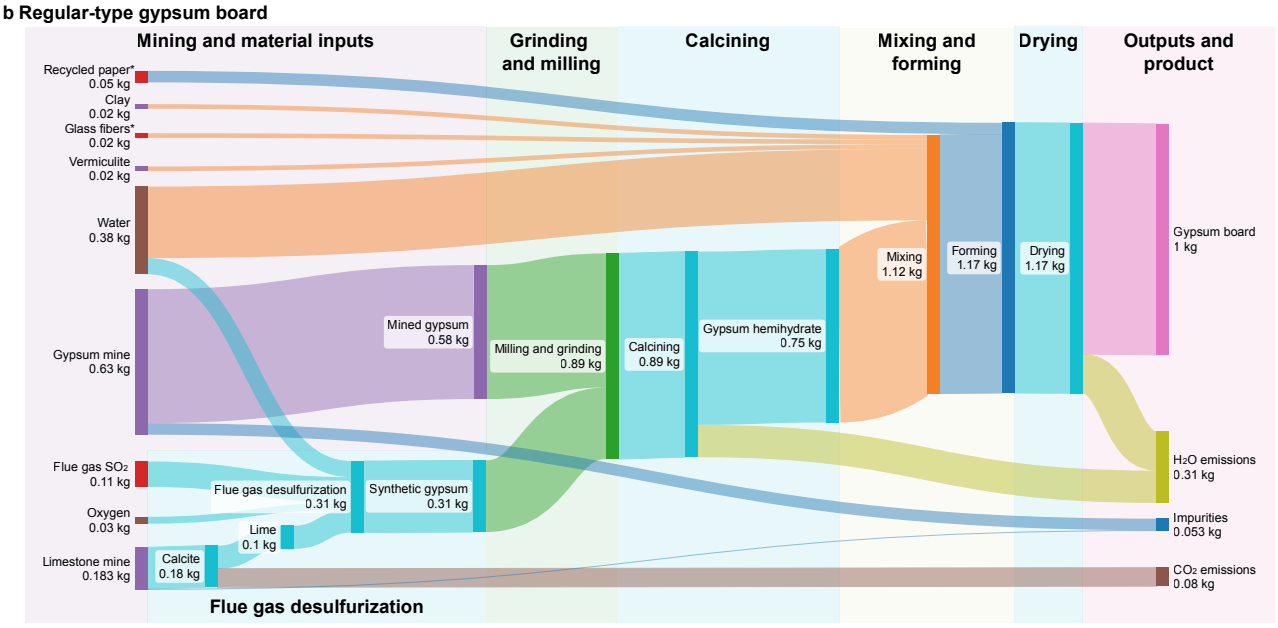


Figure 7. Sankey diagram of mass flows in (a) steel making and (b) gypsum board production. Material losses are excluded for clarity. Note that masses of coal for coking only include stoichiometrically required coke. Inputs for energy use are not shown.

The chemically derived CO₂ emissions of steelmaking are dominated by the combustion of blast furnace (1.12 kg CO₂/kg steel) and oxygen furnace (0.11 kg CO₂/kg steel) gas to CO₂ (Supplemental Figure 3a). In the scenario where these emissions are allocated to steel, they comprise 93% of all chemically derived emissions, with a total of 1.32 kg CO₂/kg of steel. Therefore, in the scenario where all these emissions are allocated to the energy product, chemically-derived emissions are greatly reduced to 0.09 kg CO₂/kg steel, driven by the calcination of limestone to form lime (0.06 kg CO₂/kg steel) and coking (0.03 kg

 CO_2 /kg steel). The system expansion allocation scenario for these emissions results in chemical-derived CO_2 emissions of 1.02 kg CO_2 /kg steel.

When all emissions are allocated to steel, steelmaking emits 2.854 kg CO₂e / kg steel, driven largely by chemical emissions from the combustion of blast furnace and oxygen furnace gases (89). Energy emissions due to blast furnace enthalpy and inefficiency in energy consumption make up most remaining emissions, and combined, these three categories comprise 85% of total GHG emissions.

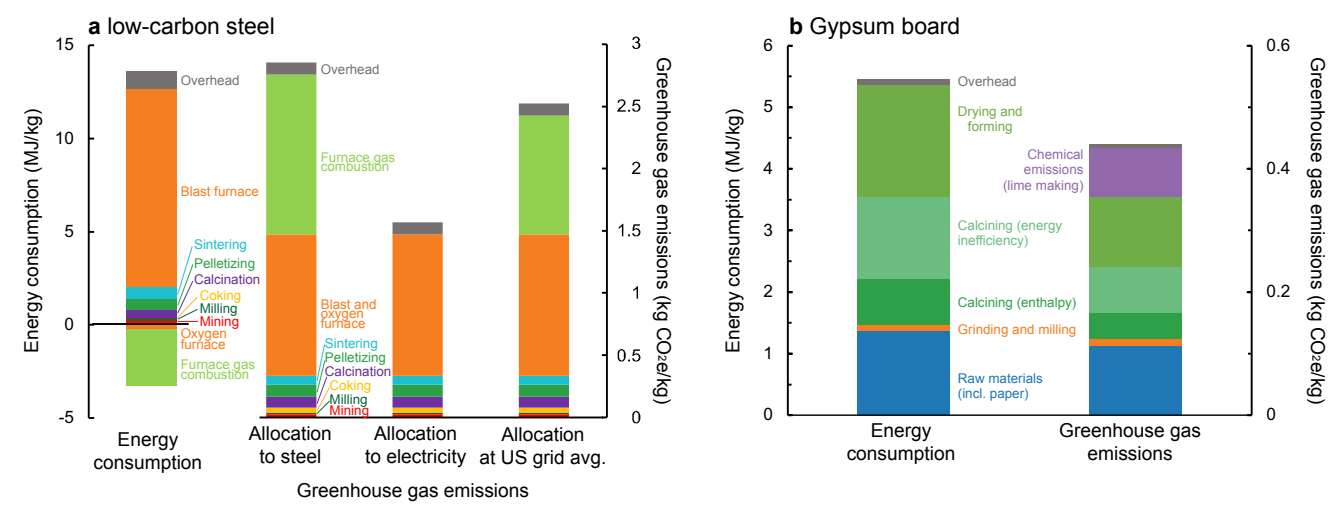


Figure 8. Energy consumption and total GHG emissions from (a) steelmaking for the three allocation scenarios considered and (b) gypsum board production.

In total, 13.7 MJ of energy is consumed to produce 1 kg of steel, and 3.3 MJ of energy is produced. Energy consumption is dominated by blast furnace enthalpy and inefficiency, which consume 78% of the total energy consumption. Produced energy is primarily due to furnace gas combustion, with only 0.27 MJ/kg steel energy being produced in the oxygen furnace, which is modeled as not recovered in all allocation scenarios.

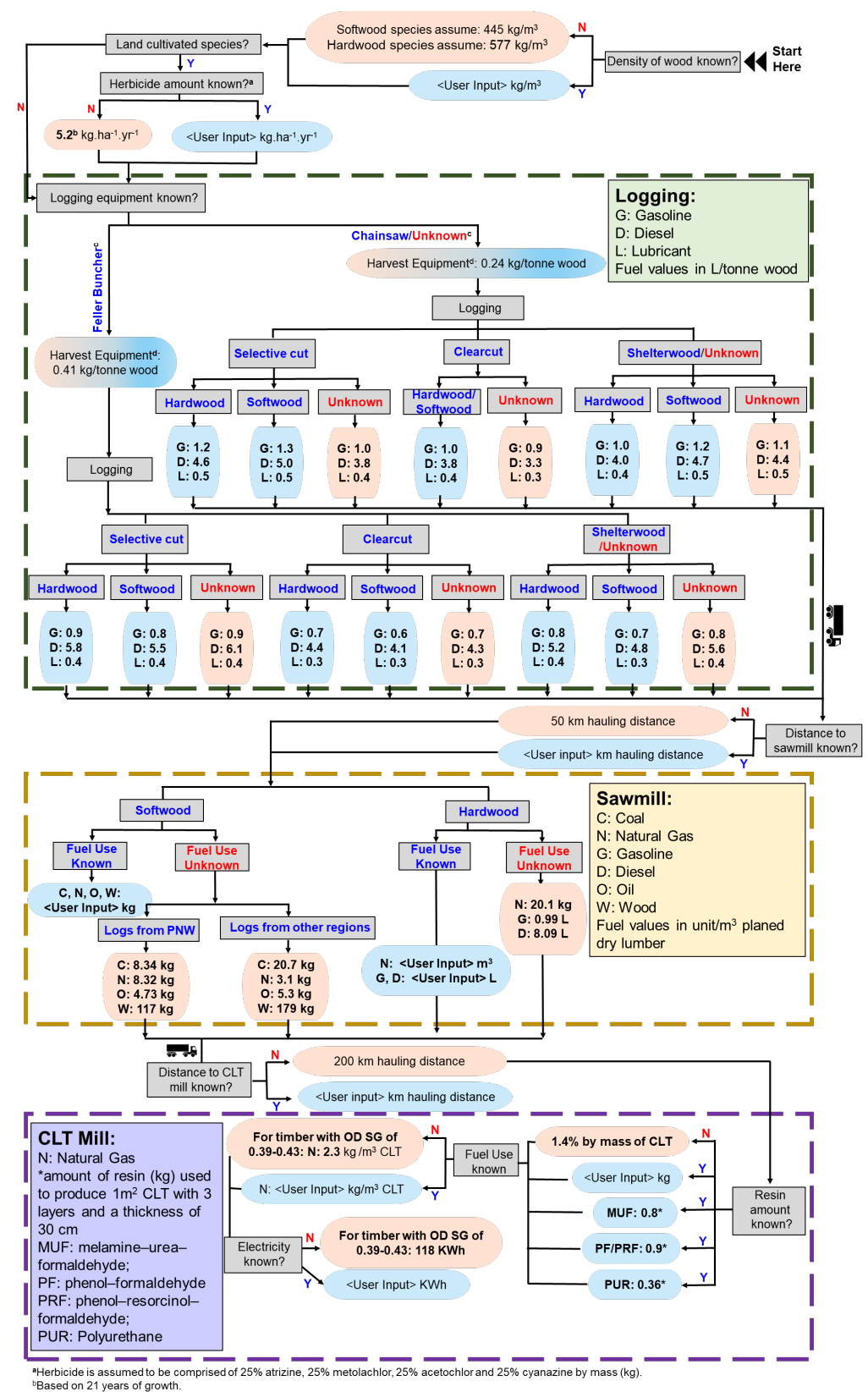
To validate the developed framework, results for steel are compared against the LCAs of steel by the IEA and Worldsteel. We make our comparison with the system expansion energy allocation for furnace gas combustion and, additionally, to match the assumptions made by these past analyses, apply system expansion to the slag co-product, considering the replacement of primary cement clinker using the GHG emissions and energy consumption determined with the ground-up model for cement. As a result of the production of 0.3 kg of slag, the GHG emissions of this scenario are reduced by 0.27 kg $\rm CO_{2e}$ / kg of steel, resulting in emissions of 2.25 kg $\rm CO_{2e}$ / kg steel. This result is comparable to emission values from both the IEA and Worldsteel of 2.2 kg $\rm CO_{2e}$ / kg steel. Total energy consumption in this scenario is modeled as 12.51 MJ / kg steel.

Gypsum board is a material used on walls that is primarily composed of a gypsum core (typically with glass fiber reinforcement) sandwiched between sheets of paper. Unlike Portland cement and low-carbon steel, where chemical conversion is the primary driver of emissions, the energy consumption of gypsum board production is primarily driven by drying processes (Supplemental Figure 4c), which account for 33% of the total energy (Figure 8b). The water content, and therefore the drying energy requirement, of gypsum board can be highly variable, depending on production facility practices, and can result in large variations in LCI data. Material inputs of recycled paper play the next largest role in energy consumption, at 60% of raw material extraction energy consumption and 15% of total energy

- 1 consumption, respectively. In this work, we considered glass and paper as already processed to
- 2 demonstrate the integration of existing LCI data for known products with the developed framework for
- 3 assessing composite materials. Due to the production of synthetic gypsum, 19% of total GHG emissions
- 4 result from chemically derived emissions, primarily the calcination of limestone to lime prior to
- 5 sulphuration, with no allocation assigned to the capture of SO₂.
- 6 The total energy consumed to produce 1 kg of gypsum board was found to be 5.46 MJ, which is in the
- 7 range of previously reported energy use of 3.44-6.74 MJ/kg gypsum board.⁶⁸⁻⁷³ In addition, variations in
- 8 kiln efficiency, paper recycling technologies, and the amount of excess water that needs to be
- 9 evaporated (e.g., when more water than required is added to aid in forming) can also cause variations in
- energy requirements. To accurately consider scenarios such as gypsum board, where evaporation (or
- other phase change reactions) plays a critical role in net emissions, careful consideration of potential
- recapture (e.g., during condensation) or use (e.g., as steam) should be made.

3.3 Complete assessment and validation of yellow poplar CLT

- 15 To validate an application to a biogenic material, we applied the framework to cross-laminated timber
- 16 (CLT) produced from YP. Typically, CLT is produced from softwoods due to their composition and
- 17 flexibility advantages and has a greater wealth of LCI data. 17,74 YP is an emerging feedstock for CLT,
- allowing for greater diversity in materials and local sourcing. Examining YP CLT enables the
- 19 framework to be applied to a more data-scarce product, thereby highlighting the framework's flexibility.
- 20 In the Supplemental Information, we have also provided the framework application to CLT from EH for
- 21 further validation of the framework. Figure 9 shows the decision tree for the ground-up analysis
- 22 performed within the framework presented in Figure 4, specifically applied to logging and forestry
- 23 practices.



off the sawmill is a medium-sized one, assume use of feller buncher-based harvesting system for logging operations. If sawmill size is unknown, or logging

Figure 9. Decision tree of the developed framework for a biogenic material grown with forestry practices.

equipment information unknown, assume use of chainsaw-based harvesting system.

*Harvesting equipment when calculating impact on GHG emissions. Mass requirements for harvesting equipment when calculating impact on GHG emissions. Mass requirements for harvesting equipment were determined by using the average equipment weight of a harvesting equipment and dividing by the lifetime anticipated harvest of 136,000 tonnes.

Here, we present results focusing on the GHG emissions for the cradle-to-gate production of 1 m³ of CLT (Figure 10). GHG fluxes are primarily tied to the energy demand and resources used. The majority of the GHG emissions are associated with the lumber production in the sawmill (~ 46% of total kg CO₂e emissions per m³ CLT), followed by the emissions associated with CLT production (~ 28% of total kg CO₂e emissions per m³ CLT). Transportation-related emissions are dependent on the routes taken by the truck and the load carrier. As such, these emissions are minimal for the haul to the sawmill (9.5 kg CO₂e/m³ CLT) and the CLT mill (6.9 kg CO₂e/m³ CLT). The energy demand results show that almost 63% of the total energy consumption occurs during the operations in the sawmill to produce lumber that serves as feedstock for the CLT mill. However, a portion of this demand is met by the renewable biomass (such as shavings and chips) generated on-site.

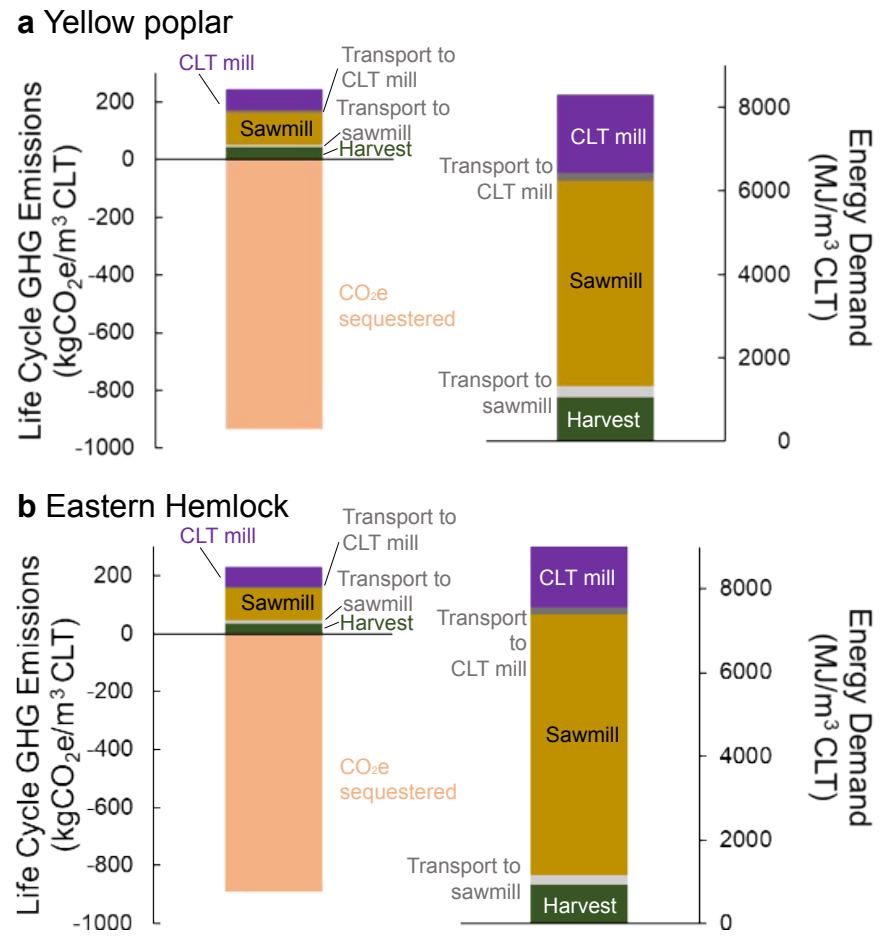


Figure 10: Life Cycle Greenhouse Gas Emissions and Energy Demand for the cradle-to-gate production of 1 m³ CLT using (a) YP and (b) EH as a source of wood.

3.1.6 Accounting for biogenic carbon

CLT stores 933 kg $CO_{2}e$ / 1 m³ based on a carbon content of 50% of the wood. As a result, the net cradle-to-gate GHG emissions are approximately -691 kg $CO_{2}e$ / m³ CLT.

The GHG emissions modeled herein for CLT are consistent with previously published results, ^{17,60,62} with slight variations due to the difference in the source of the lumber. GHG emissions are primarily a function of energy demand, and our energy demand results for the sawmill operations stage (4932 MJ / m³) are higher than results published in some sources, ^{17,62} but are in agreement with the previously

published energy demand data for Southeast (SE) region lumber production (reported as 5151 MJ/m³ dry lumber);³⁰ our results are within 4% of this value. This variation may be due to the approximations used in this study, which are based on the North American Electric Reliability Corporation's SERC region electricity grid mix and YP as the source of lumber. However, the US electric grid mix is well characterized for all states, and the US average grid mix could be used to estimate emissions for a generalized case study. Additionally, the use of facility-specific equipment and processes (such as the use of chainsaws and a clear-cut method for logging operations rather than feller buncher-based felling operations and the shelterwood method of thinning assumed in this study) can be integrated into this framework if material producers seek more specific results.

3.4 Challenges presented by other biogenic materials

Due to the wide variety of potential biogenic materials and product types, LCA researchers should closely consider the variations we have outlined in the framework and highlighted in the case study of YP CLT. As shown in Figure 10 of the case study results, carbon sequestered via photosynthetic growth can substantially impact the results and can have the greatest amount of variability. When assessing a biogenic product, researchers should consider using a range of sequestration values, as illustrated in past work⁷⁵ and tabulated in Supplemental Table 2. Sawmill processing and manufacturing of CLT represent the second-largest contributions to life-cycle impacts for CLT, highlighting mechanical processing as a key focus area for emissions reduction during wood processing. For many wood products, representative process data is available for mechanical processes, and when not available, a ground-up approach considering fuel use, equipment, yield, and energy efficiency can be taken as demonstrated in this work. Biomass growth and harvesting are considered from the ground-up in this work emissions; however, further considerations such as land-use changes that may play a critical role in LCA results are not considered.

The developed framework focused on forestry, as forest products represent most of the biogenic material used industrially. A similar approach could be taken for agricultural crops by considering appropriate energy inputs for cultivation and harvesting, as well as fertilizer, herbicide, and other inputs to agricultural feedstocks to develop a similar ground-up calculation to those developed herein for forestry and logging. Growth of biomass in greenhouses may need to consider heating or ventilation requirements of the structure alongside these factors, which are specific to the climate in which the crop is grown. In cases where exact supply chains for the material production are not known, uncertainty assessment may be utilized to consider a variety of scenarios for resource procurement and inform distributions of anticipated impacts. When considering materials produced from agricultural residues or other waste products (e.g., biosolids, food waste), critical consideration of different approaches to allocation of upstream impacts to the resulting product should be made, as in conventional LCA. This consideration should occur alongside of development of a ground-up approach to quantify LCI data for process steps for the collection and processing of these materials if unavailable.

 Beyond forestry and agriculture, an adapted approach could be taken for the growth of marine biomass (such as algae or seaweed) for use in biofuel processes or materials, considering the chemical composition of these materials and net carbon uptake. In cases such as growth of algae in bioreactors, a combined approach considering composition of the resulting algae, ground-up assessment of process inputs from sub-process requirements, and thermodynamic modeling of heat required for the process could be utilized to estimate LCIs via development of an approach considering both chemical first principles and ground-up process modeling. Other resources, such as fungal biomass, may require consideration of input resources, such as growth media, and LCIs of those resource may be available, or need to be developed. Given the diversity of potential biomass growth pathways, this work is limited in

its consideration of only forestry products, however the ground-up approach developed herein could be expanded by future practitioners to include other raw resources to better estimate LCIs in data-poor environments.

3 4 5

6

7

8

9

10

11

1

2

Some biogenic materials may undergo chemical processing after production, for example, in the production of paper, bioethanol, bio-based plastics, or bio-based carbon materials. The complex structure of biomass constituents, such as hemicellulose and lignin, can make modeling of chemical conversion complex, particularly for highly novel conversion processes. In these cases, to apply the methods developed for chemical conversion within this framework it may be necessary to collect experimental data on the thermodynamics of the chemical reaction used for chemical conversion. For many reactions, it may be possible to model the thermodynamics of chemical conversion based on bulk constituent processes, as has been applied in past work to estimate LCIs for pyrolysis.⁷⁶

12 13 14

15

16

17 18

19

20

21

22

23

24

25

26

27

28 29

30

31

32

33

34

35

36

37

3.5 Integrating uncertainty and sensitivity analysis

A key benefit of the combined ground-up and first principles approach developed in this work is that uncertainty and sensitivity analyses can be integrated at the parameter level to consider variation or uncertainty that may result from processes, while maintaining the certainty in underlying, first principles-derived values. For example, during cement pyroprocessing, uncertainty in material losses or thermal efficiency could be considered as individual parameters, rather than applying a blanket uncertainty to the whole process for energy consumption or material flows. Using this example, critically uncertain parameters in our examination of cement production with the developed framework include material losses during production and thermal efficiency. Process parameters for these components of the framework would be expected to be more uncertain when examining novel materials. To examine this uncertainty, we utilized a sensitivity analysis examining a range of material losses and thermal efficiency. For material losses we considered a range from 1% for each process step except storage at 0.33%, for 4.4% material loss across the entire production, to 5% for each process step, except storage at 1.67% for 23.6% material loss across the whole process. For thermal efficiency, we considered a range from 26.5%, representative of a wet kiln⁷⁷ to 63%, representative of a highly efficient dry kiln with preheater and pre-calciner. 77 This analysis shows a decrease of 0.011 kg CO₂e/kg cement for each percentage increase in thermal efficiency, and it results in an increase of 0.0049 kg CO₂/kg cement for each percentage material loss across the whole process cycle, noting that this would differ with different distributions of material loss (Supplemental Figure 5). Additionally, when considering biogenic building materials, uncertainties may arise due to potential variability in growth conditions, regional variability and environmental conditions. For instance, a cradle-to-grave life cycle GHG emissions of 317 to 333 kg CO₂e/m³ CLT is emitted for softwood, when varying the source of wood.⁷⁵ When applied to novel materials production, such an approach can be utilized to examine the likelihood that a novel material production pathway, changes in material production parameters, or shifts in resources used would result in reductions in emissions, compared to conventional practices.

38 39

40

41

4. Discussion

4.1 Application of this framework to novel materials

- We have validated the developed framework against conventional Portland Cement, low-carbon steel,
- 43 gypsum board, and two types of CLT. However, the primary application of this methodology is expected
- 44 to be novel building materials and identifying low or negative-carbon materials that may aid
- 45 infrastructure in transitioning from net carbon-emitting to net carbon-sequestering. To aid in utilizing the
- developed decision tress for specific materials, we discuss here specific challenges with application of
- 47 this framework to novel materials, including example sources of uncertainty in chemical conversion,

1 thermal efficiency, and resource extraction, pathways for integration of uncertainty assessment, and

2 development of ground-up inventories for mineral derived materials.

29

30

3132

33

34

35

36

37

38

39

40

41

42

43 44

45

3 For materials involving chemical conversion, key considerations are process enthalpy and thermal 4 efficiency. Process enthalpy may be challenging to determine when reactions are complex, poorly 5 characterized, or enthalpy of formation of reactants has not been previously determined. Thermal 6 efficiency of a commercial scale system may be challenging to estimate if data are not available for 7 similar systems. In cases such as these, a tiered approach should be taken to consider thermal efficiency, 8 considering first a representative commercial scale alternative if available. When available thermal 9 efficiencies from analogous commercial systems can serve as proxies, for example utilizing existing 10 cement production efficiency in a comparative assessment of alternative clinker cement binders. 12 If commercial scale thermal efficiency is unavailable for a similar system, a distribution of pilot or lab 11 12 scale data could be used, to represent potential variability in such data. For example, in prior work on poplar biochar production via pyrolysis, ⁷⁸ where commercial-scale efficiencies were unavailable, a 13 14 distribution of 38 literature values was used to represent potential variability in thermal efficiency. In 15 other cases, if no similar commercial systems or experimental data exist, sensitivity of results to process 16 thermal efficiency should be carefully considered across a wide range, as shown in Supplemental Figure 17 5 for cement, to determine the likelihood a novel technology reduces emissions compared to existing 18 alternatives. For most novel materials, experimental data define composition and synthesis pathways, 19 enabling estimates of resource demand, enthalpy of formation, and reaction-based emissions. If exact 20 composition is unknown, it can be approximated using representative compounds (e.g., a majority 21 mineral phase present in an ore) or bulk averages (e.g., biomass cellulose, hemicellulose and lignin 22 constituents ⁷⁶). Some processes may rely on poorly characterized minerals or phases, requiring new 23 enthalpy data, such as determination consideration of varying feedstock mineralogy or sourcing between 24 lab and commercial scales. Such uncertainty may require consideration and comparison of multiple 25 potential pathways to materials production. While such analysis increases the complexity and time of a 26 required analysis, the developed framework provides the ability to isolate the process steps that may be 27 more uncertain, allowing for additional focus on these steps and their downstream effects, while limiting 28 repeated analysis.

Resource extraction could be a major source of uncertainty in inventories for novel materials that utilize resources or extraction techniques that lack existing LCI data. Herein, we developed a ground-up approach for forestry practices to address this data gap in LCI development in data-poor environments. To model mining and quarrying when high quality, comparable LCI data do not exist, a similar groundup approach could estimate energy use based on mineral hardness, extraction depth, and mining methods. Considering these processes from the ground-up could be applied to either existing mining practices, such as open pit, strip, or underground mining, by considering the equipment used for each technique, their fuel consumption, depth of the ore extracted, and amount of ore extracted per unit of the desired mineral, as well as allocation to mining co-products. As was exemplified herein for forestry and sawmilling, considering energy usage of similar processes and differences in fundamental process parameters between those processes and novel processes could be performed utilizing these parameters to examine novel mining processes from the ground-up. Novel processes to extract minerals, such as through desalination⁷⁹ or biomineralization⁸⁰, may utilize hybrid methods to model chemical conversion and separation processes as part of the resource extraction modeling, considering both ground-up and first principles approaches to develop such sub-process inventories. Some novel material production pathways may use fungal-81 or microbial-derived82 materials, which may require expansion of the principles developed in this framework to apply.

Uncertainties in process efficiency, material yield and losses, and facility overhead necessitate probabilistic assessments, even in LCA of well-established systems, such as cement production. When parameters are highly uncertain, or when existing similar systems have high variation, integration of the framework provided with uncertainty assessment can estimate the likelihood that a proposed technology results in a reduction in emissions, compared to current practice, given a range of material production values (e.g., thermal efficiency, resource purity, or resource extraction methods or sources). Such assessment can allow for highly uncertain pathways to materials production to be quantitatively compared, while considering potential data scarcity at different levels of development.

Additional processing steps (e.g., forming) can be modeled with first-principles methods, such as estimating steel casting energy from melt enthalpy and heat transfer.⁸⁴ The energy requirement of process steps involving chemical conversion other than chemical reactions, such as cooling, phase change, or separation reactions, may be more accurately modeled with other methods, such as Gibbs free energy minimization, which have previously been utilized and examined for developing LCIs for chemical production.¹⁴ We note that beyond those discussed herein, there may be additional challenges that are not addressed by this framework, as the process steps taking in novel processes are inherently unknown. This framework does not prescribe exact methods for every case but provides a generalizable approach to refine first-principles LCIs, reduce data gaps, and complement process-simulation models.

4.2 Comparison to past approaches for estimating LCI data

Past studies have utilized aspects of the framework proposed herein to assess individual materials or products. For example, past studies have considered first principles approaches combined with process calculations, as in the work developed herein, to be intermediate in both accuracy and data requirement. This pathway offers improved accuracy compared to just considering stoichiometry and reduced data requirements than full process simulation, as in software such as Aspen Plus.¹⁰ We note that the ground-up approach to resource extraction developed herein expands beyond what has been done in these past studies, to consider a pathway to estimate these process steps, rather than relying on existing databases for upstream impacts (Table 1).

Past studies utilizing first principles and ground up methods have typically found results in agreement with other methods to estimate LCIs. ¹⁰ Many of these past studies have focused on the assessment of individual materials (Table 1), rather than a generalizable approach to estimate such data. Such approaches may result in a more accurate assessment of an individual material, but they may not broadly facilitate representative comparisons between different production pathways. These studies all apply differing methodologies to estimate missing data, with some studies utilizing first principles, some a constant value for the missing parameter, and some utilizing machine learning or other methods to fill data gaps. ^{10,12,14,85} The framework developed by Yao and Masanet provides additional guidance for the analysis of chemical production from first principles, including detailed modeling of separation, evaporation, crystallization and adsorption processes, offering more detail on novel process modeling steps than the work presented herein. ¹⁴ Yet past studies have not provided a systematic approach that can be broadly compared across materials, particularly including guidance on analysis of material extraction, and integrating mechanisms to address extraction, reaction, and manufacturing processes with the flexibility for quantifying variation and uncertainty in individual inputs as was done herein.

Study	Resource extraction	Mechanical processing	Chemical separation	Chemical conversion	Transportation	Materials considered
Miller and Myers, 2019 ¹²	Existing databases for material specific resources	Existing commercial process	N/A	First principles and existing commercial process thermal efficiency	Constant	Alternative cements
Parvatker and Eckelman, 2019 ¹⁰	Existing databases	Process calculations	First principles	First principles, assumed thermal efficiency	N/A	Styrene
Wernet, Hellweg, and Hungerbühler, 2012 ¹³	N/R	N/A	N/R	Constant energy use, constant yield or machine learning	Constant	Polyvinyl chloride, tobacco flavor
Yao and Masanet, 2018 ¹⁴	Previous data	Based on motor used	First principles	First principles, technology specific thermal efficiency	Constant	Chemical production
Framework developed herein	Ground-up approach to estimate resource extraction	Bond's equation for crushing, ground-up approach for other processes	First principles, existing efficiency estimates	First principles, existing commercial thermal efficiency estimates for similar technologies	Constant	Materials production

When differing approaches are taken to estimate LCIs in a data-poor environment, it can bias the results, depending on the approach taken. 86 When identifying pathways to decarbonization of industry broadly, multiple technologies must be considered, across numerous material types, and comparisons at a broad level, even for many specific novel materials are facilitated by this framework.

Some studies have relied on different thermodynamic methods to estimate energy of chemical conversion and separation steps, such as exergy^{87,88} and Gibbs free energy minimization.⁸⁹ We note that while enthalpy was used herein, the developed framework does not exclude the use of other pathways to estimate energy if appropriate for a novel system, by substituting such analyses at appropriate steps. However, consideration should be made for limited data availability characterizing thermodynamics for even common compounds, particularly for exergy, which may make such analysis difficult for novel production pathways, and may require experimental determination of such values.⁸⁷

4.3 Limitations and expansion of framework application

The primary role of the framework developed herein was to provide a step-by-step, repeatable process for determining the life cycle GHG emissions of novel materials and processes in data-poor environments. This framework is currently limited in its examination of only GHG emissions/uptake and energy consumption. Building on this framework, similar methods could be applied to determine other life-cycle impacts, but development of such an approach may be challenging for impacts that are highly dependent on exact facility practices, such as particulate matter emissions. Knowledge of material reactions can be applied to determine other outputs to the environment from chemical reactions (e.g., SO₂ in roasting of metal sulfide ores) and similar combinations of existing LCIs for known processes, as well as modeling novel processes from first principles. Some emissions, such as particulate emissions, may be particular to facility design or operation conditions. In these cases, standard proxy or estimation methods should be used. These methods will provide similar data quality to existing methods, while data

quality for methods that can be accurately modeled with first-principle or ground-up LCI will be improved by the developed framework.

When high quality facility specific data can be collected, representative LCI database entries exist, or sufficient process details exist for full process simulation, the approach developed herein does not replace these methods, which are expected to be more accurate when required data are available.¹⁰ Instead, this approach serves to bridge between simple first-principles calculations and full process simulation, while the ground-up approach to resource extraction improves on using proxy or non-region specific data for these process steps, when specific LCI data is not available. Other approaches, such as utilizing artificial intelligence or machine learning techniques could be used to estimate LCI data at similarly low data levels as required by the herein developed framework. 85,90,91 However, such approaches require large datasets to train, and while this may be viable for some material types, such as the training on molecular structures to predict chemical LCIs, 85 such data for training of models may not be available for all novel material types, and mismatched data may introduce concerns with overfitting. A limitation of this work is that future novel technologies are inherently unknown, and a framework cannot be devised to encompass all possible material production pathways. In these cases, this framework, along with other works such as the framework developed by Yao and Masanet for developing LCIs of chemicals, 14 can provide guidance on development of such assessments as well as allowing comparison to existing production pathways. Existing known pathways to produce materials, such as biomineralization, microbial production of bioplastics, or fungal insulation materials, may require meaningful expansion of the scope of the framework as currently developed, limiting its application to these diverse material production pathways without additional expansion. However, future work could utilize the principles of the herein developed similarly detailed framework to determine LCIs for such materials.

For biogenic materials, novel materials present significant data challenges that can be overcome with the developed ground-up approach, particularly in the stages that will contribute the most to life-cycle impacts (i.e., carbon storage, processing, manufacturing). Our case study application of YP CLT reflects an emerging feedstock for CLT production, where data challenges were significant in processing and manufacturing. Working with existing similar facilities directly to obtain primary data and validating this approach with YP material experts allowed this framework to reduce uncertainties for this novel lumber material. Since novel biogenic materials can come from a wide variety of feedstocks, future framework applications should determine early in the assessment process where data gaps are most significant and begin to contact experts and practitioners to obtain primary or (in the case of missing data) proxy data to start mitigating uncertainties and data gaps early in the process.

4.4 Policy and commercial application

There have been numerous efforts around the world to integrated embodied carbon assessments into policies (e.g., for public procurement and building applications⁹²) and into commercial practice (e.g., to meet corporate sustainability goals⁹³). In data-poor environments, such as early in the development process, comparison of novel technologies for reducing GHG emissions may be challenging due to differences in considered scope, scale, and limited reporting on exact material properties. Many policies require assessment of the emissions of the materials used, for example, as in whole-life carbon disclosure, ⁹⁴ Buy Clean procurement requirements, ⁹⁵ emissions intensity requirements, ⁹⁶ or border carbon adjustments. ⁹⁷ These policy mechanisms often require production of an environmental product declaration (EPD), which would require data that may be unavailable at pilot scale. As such, policy mechanisms to encourage the use of novel low-carbon materials or promote their development require data, such as the herein developed ground-up framework, to assess material emissions early in the

development process. Further, early adopters of low-carbon or net-uptake materials may have multiple alternatives to reduce emissions, and when those materials have been examined with different scopes or LCA methodologies, verifying and comparing estimates for emissions of data-poor materials can be challenging. In such cases, integration of the framework developed herein with uncertainty assessment, as detailed previously,^{78,83} can create a probabilistic assessment of the likelihood of emissions reduction with a given technology with a range of technology development pathways. The developed framework can aid in providing a unified analysis for comparing novel, low or negative carbon materials by policy makers and early adopters to aid in driving adoption of these materials, while ensuring materials do result in reduced or negative emissions.

As an example of such application, in assessment of reducing the emissions of concrete binder production, a comparison could be made between improvements in process efficiency of Portland cement production and switching to an alternative binder, such as a carbonatable calcium silicate cement. 12 If the improvements in process efficiency of an existing facility for Portland cement followed our sensitivity analysis (Sec. 3.5), paired with a switch to natural gas as the sole fuel source, it would result in a 0.18 kg CO₂e/kg cement reduction in GHG emissions, with a majority (0.53 kg CO₂e/kg cement) of the remaining 0.75 kg CO₂e/kg cement GHG emissions being driven by chemical-derived emissions. In contrast, a switch to the alternative binder carbonatable calcium silicate cement, while maintaining the original process efficiency and fuel mix, would reduce these chemical-derived emissions to 0.38 kg CO₂e/kg cement, while also reducing the enthalpy of reaction required from 1.7 MJ / kg Portland cement to 0.77 MJ / kg carbonatable calcium silicate cement. 12 As a result, such a system would reduce total emissions to 0.63 kg / kg cement, a greater reduction than from efficiency improvements to Portland cement. Notably, this simple example excludes implementation concerns such as resource availability, implementation, and material property differences. Such analysis can be paired with other data available early in the development process to aid in decision making regarding scale up and further investment in technologies to reduce or store CO₂ emissions. Such analysis could further be paired with distributions of likely process parameters (e.g., thermal efficiency) to develop distributions of outcomes for different decarbonization strategies, ^{78,83} or paired with local or global resource assessments to estimate how best to utilize potentially limited resources to achieve decarbonization goals.

 As novel materials, systems, and products continue to be developed to decarbonize industrial sectors, the framework presented herein can help to address critical data gaps in LCI data early in the research and development process. By providing a systematic method to improve the accuracy of first-principle LCIs, GHG emissions are critical data for industrial decarbonization that can be estimated for novel materials. The framework developed in this work provides a generalizable approach to developing LCIs for broad classes of materials in data-poor environments, allowing for comparison between differing technologies. This framework builds on past approaches to holistically consider material production from cradle-togate, inclusive of approaches to estimate LCI data for raw resource extraction process steps lacking existing LCI data, to better fill data gaps for novel materials production. We believe this framework has broad applicability to the development of novel materials for broad applications, including decarbonizing building materials, carbon sequestration in materials, biofuels, and bioproducts, and the development of novel energy materials and technologies.

Acknowledgements

- 46 S.K., J.F., B.B., T.H., C.D.S., and S.M.'s contribution to this work was funded through the US
- 47 Department of Energy, Advanced Research Projects Agency-Energy (ARPA-E, Grant #DE-
- 48 AR0001625). This article represents the views of the authors, not necessarily those of the funder. This

- work was supported in part by the U.S. Department of Energy, Office of Science, Office of Biological
- 2 and Environmental Research, through contract DE-AC02-05CH11231 between Lawrence Berkeley
- 3 National Laboratory and the U.S. Department of Energy. The U.S. Government retains and the
- 4 publisher, by accepting the article for publication, acknowledges that the U.S. Government retains a
- 5 nonexclusive, paid-up, irrevocable, worldwide license to publish or reproduce the published form of this
- 6 manuscript, or allow others to do so, for U.S. Government purposes.

References

7 8

9

- 1 S. Kane and S. A. Miller, Greenhouse gas emissions of global construction material production, *Environmental Research: Infrastructure & Sustainability*.
- 2 E. G. Hertwich and R. Wood, The growing importance of scope 3 greenhouse gas emissions from industry, *Environmental Research Letters*, 2018, **13**, 104013.
- National Academies of Sciences, Engineering, and Medicine, Gaseous Carbon Waste Streams
 Utilization: Status and Research Needs, National Academies Press, 2019.
- 4 E. Van Roijen, S. A. Miller and S. J. Davis, Building materials could store more than 16 billion tonnes of CO2 annually, *Science*, 2025, **387**, 176–182.
- 5 Organisation for Economic Co-operation and Development (OECD), *Global Material Resources Outlook to 2060: Economic Drivers and Environmental Consequences*, 2019.
- 19 6 International Energy Agency, Material efficiency in clean energy transitions, 2019.
- 7 J. L. Rivera and J. W. Sutherland, A design of experiments (DOE) approach to data uncertainty in LCA: application to nanotechnology evaluation, *Clean Techn Environ Policy*, 2015, **17**, 1585–1595.
- 8 F. Piccinno, R. Hischier, S. Seeger and C. Som, From laboratory to industrial scale: a scale-up framework for chemical processes in life cycle assessment studies, *Journal of Cleaner Production*, 2016, **135**, 1085–1097.
- 9 S. Zargar, Y. Yao and Q. Tu, A review of inventory modeling methods for missing data in life cycle assessment, *Journal of Industrial Ecology*, 2022, **26**, 1676–1689.
- 10 A. G. Parvatker and M. J. Eckelman, Comparative Evaluation of Chemical Life Cycle Inventory
 Generation Methods and Implications for Life Cycle Assessment Results, ACS Sustainable Chem.
 Eng., 2019, 7, 350–367.
- 30 11 N. von der Assen, J. Jung and A. Bardow, Life-cycle assessment of carbon dioxide capture and utilization: avoiding the pitfalls, *Energy Environ. Sci.*, 2013, **6**, 2721–2734.
- 32 12 S. A. Miller and R. J. Myers, Environmental Impacts of Alternative Cement Binders, *Environmental Science and Technology*, 2020, **54**, 677–686.
- 13 G. Wernet, S. Hellweg and K. Hungerbühler, A tiered approach to estimate inventory data and impacts of chemical products and mixtures, *Int J Life Cycle Assess*, 2012, **17**, 720–728.
- 14 Y. Yao and E. Masanet, Life-cycle modeling framework for generating energy and greenhouse gas
 emissions inventory of emerging technologies in the chemical industry, *Journal of Cleaner Production*, 2018, 172, 768–777.
- 15 J. L. Hau, H. Yi and B. R. Bakshi, Enhancing Life-Cycle Inventories via Reconciliation with the Laws of Thermodynamics, *Journal of Industrial Ecology*, 2007, **11**, 5–25.
- 16K. Sahoo, R. Bergman and T. Runge, Life-cycle assessment of redwood lumber products in the US,
 Int J Life Cycle Assess, 2021, 26, 1702–1720.
- 17C. X. Chen, F. Pierobon and I. Ganguly, Life Cycle Assessment (LCA) of Cross-Laminated Timber
 (CLT) Produced in Western Washington: The Role of Logistics and Wood Species Mix,
 Sustainability, 2019, 11, 1278.
- 18 Y. Wang, R. Rasheed, F. Jiang, A. Rizwan, H. Javed, Y. Su and S. Riffat, Life cycle assessment of a
 novel biomass-based aerogel material for building insulation, *Journal of Building Engineering*, 2021,
 44, 102988.

- 1 19J. Pett-Ridge, S. Kuebbing, A. C. Mayer, S. Hovorka, H. Pilorgé, S. E. Baker, S. H. Pang, C. D.
- Scown, K. K. Mayfield and A. A. Wong, Roads to removal: options for carbon dioxide removal in
- the United States, Lawrence Livermore National Laboratory (LLNL), Livermore, CA (United States),
 2023.
- 5 20 N. Kunert and L. M. T. Aparecido, Ecosystem carbon fluxes are tree size-dependent in an Amazonian old-growth forest, *Agricultural and Forest Meteorology*, 2024, **346**, 109895.
- 7 21 B. Hirel, T. Tétu, P. J. Lea and F. Dubois, Improving Nitrogen Use Efficiency in Crops for Sustainable Agriculture, *Sustainability*, 2011, **3**, 1452–1485.
- 9 22 Argonne National Laboratory, *Greenhouse gases, Regulated Emissions, and Energy use in Technologies (GREET)*, US Dept. of Energy, 2023.
- 23 R. Morales-Vera, L. Vásquez-Ibarra, F. Scott, M. Puettmann and R. Gustafson, Life Cycle
- Assessment of Bioethanol Production: A Case Study from Poplar Biomass Growth in the U.S. Pacific Northwest, *Fermentation*, DOI:10.3390/fermentation8120734.
- 24 P. D. Miles and W. B. Smith, Specific gravity and other properties of wood and bark for 156 tree
 species found in North America, Res. Note NRS-38. Newtown Square, PA: U.S. Department of
 Agriculture, Forest Service, Northern Research Station. 35 p., 2009, 38, 1–35.
- 25 D. Abbas and R. M. Handler, Life-cycle assessment of forest harvesting and transportation operations in Tennessee, *Journal of Cleaner Production*, 2018, **176**, 512–520.
- 19 26G. Wernet, C. Bauer, B. Steubing, J. Reinhard, E. Moreno-Ruiz and B. Weidema, The ecoinvent database version 3 (part I): overview and methodology, *Int J Life Cycle Assess*, 2016, **21**, 1218–1230.
- 21 27 National Renewable Energy Laboratory, U.S. Life Cycle Inventory Database, 2012.
- 22 28 S. Kane and S. A. Miller, Mass, enthalpy, and chemical-derived emission flows in mineral processing, *Journal of Industrial Ecology*, 2024, **28**, 469–481.
- 24 29 F. C. Bond, Crushing & Grinding Calculations Part 1, *British Chemical Engineering*, 1961, **6**, 378–385.
- 30 M. Milota and M. Puettmann, Life Cycle assessment for the cradle-to-gate production of softwood lumber in the PNW and SE regions, *Forest Products Journal*, DOI:10.13073/FPJ-D-16-00062.
- 31 S. S. Hubbard, R. D. Bergman, K. Sahoo and S. A. Bowe, A life cycle assessment of hardwood lumber production in the northeast and north Central United States, *CORRIM Report.* 45 p., 2020, 1–45.
- 31 32 J. de Bakker, Energy Use of Fine Grinding in Mineral Processing, *Metallurgical and Materials* 32 *Transactions E*, 2014, **1**, 8–19.
- 33 N. L. Weiss, *Particle Characterization, Mineral Processing Handbook*, American Insitute of Mining and Metallurgy, 1985.
- 35 34 US Dept. of Energy Advanced Manufacturing Office, Manufacturing Energy and Carbon Footprints
 36 (2018 MECS), 2021.
- 35 Wade A. Amos, *Report on Biomass Drying Technology*, National Renewable Energy Lab, 1998.
- 38 36U.S. Environmental Protection Agency, Greenhouse Gas Inventory Guidance Direct Emissions from
 39 Stationary Combustion Sources, 2016.
- 40 37 A. Messmer, MSc Tehesis., ETH Zurich, 2015.
- 38 S. C. Davis and R. G. Boundy, *Transportation Energy Data Book*, Oak Ridge National Laboratory, 39th edn., 2021.
- 43 39 United States Geological Survey, 2019.
- 44 40 M. L. Marceau, M. A. Nisbet and M. G. VanGeem, *Life Cycle Inventory of Portland Cement Concrete*, Portland Cement Association, 2007.
- 46 41 D. Harrison, A. Bloodworth, J. Eyre, P. Scott and M. MacFarlane, Utilisation of mineral waste: a scoping study, *British Geological Survey*.
- 48 42 C. Mitchell, *Quarry Fines and Waste*, British Geological Survey, 2009.

- 43 NSF, Product Category Rule for Environmnetal Product Declarations: PCR for Concrete., 2019.
- 2 44D. N. Huntzinger and T. D. Eatmon, A life-cycle assessment of Portland cement manufacturing:
- comparing the traditional process with alternative technologies, *Journal of Cleaner Production*, 2009,
 17, 668–675.
- 5 45 N. V. Y. Scarlett, I. C. Madsen, L. M. D. Cranswick, T. Lwin, E. Groleau, G. Stephenson, M.
- 6 Aylmore and N. Agron-Olshina, Outcomes of the International Union of Crystallography
- Commission on Powder Diffraction Round Robin on Quantitative Phase Analysis: samples 2, 3, 4,
- 8 synthetic bauxite, natural granodiorite and pharmaceuticals, *J Appl Cryst*, 2002, **35**, 383–400.
- 9 46 S. Kaufhold, M. Hein, R. Dohrmann and K. Ufer, Quantification of the mineralogical composition of clays using FTIR spectroscopy, *Vibrational Spectroscopy*, 2012, **59**, 29–39.
- 47 J. Karni and E. Karni, Gypsum in construction: origin and properties, *Materials and Structures*, 1995,
 28, 92–100.
- 48 Lu, Liming, Iron Ore Mineralogy, Processing and Environmental Sustainability, Elsevier, 2nd edn.,
 2021.
- 49 P. Šiler, I. Kolářová, J. Bednárek, M. Janča, P. Musil and T. Opravil, The possibilities of analysis of
 limestone chemical composition, *IOP Conf. Ser.: Mater. Sci. Eng.*, 2018, 379, 012033.
- 50 F. Vegliò, B. Passariello and C. Abbruzzese, Iron Removal Process for High-Purity Silica Sands Production by Oxalic Acid Leaching, *Ind. Eng. Chem. Res.*, 1999, **38**, 4443–4448.
- 51 A. Kim, P. R. Cunningham, K. Kamau-Devers and S. A. Miller, OpenConcrete: a tool for estimating the environmental impacts from concrete production, *Environ. Res.: Infrastruct. Sustain.*, 2022, **2**, 041001.
- 52 J. Li, W. Zhang, C. Li and P. J. M. Monteiro, Eco-friendly mortar with high-volume diatomite and fly ash: Performance and life-cycle assessment with regional variability, *Journal of Cleaner Production*, 2020, **261**, 121224.
- 53 C. D. Scown, A. A. Gokhale, P. A. Willems, A. Horvath and T. E. McKone, Role of Lignin in
 Reducing Life-Cycle Carbon Emissions, Water Use, and Cost for United States Cellulosic Biofuels,
 Environ. Sci. Technol., 2014, 48, 8446–8455.
- 54N. R. Baral, O. Kavvada, D. Mendez Perez, A. Mukhopadhyay, T. S. Lee, B. A. Simmons and C. D.
 Scown, Greenhouse Gas Footprint, Water-Intensity, and Production Cost of Bio-Based Isopentenol as
 a Renewable Transportation Fuel, ACS Sustainable Chem. Eng., 2019, 7, 15434–15444.
- 55B. Neupane, N. V. S. N. M. Konda, S. Singh, B. A. Simmons and C. D. Scown, Life-Cycle
 Greenhouse Gas and Water Intensity of Cellulosic Biofuel Production Using Cholinium Lysinate
 Ionic Liquid Pretreatment, ACS Sustainable Chem. Eng., 2017, 5, 10176–10185.
- 56H. M. Breunig, J. Amirebrahimi, S. Smith and C. D. Scown, Role of Digestate and Biochar in Carbon-Negative Bioenergy, *Environ. Sci. Technol.*, 2019, **53**, 12989–12998.
- 36 57 S. L. Nordahl, J. P. Devkota, J. Amirebrahimi, S. J. Smith, H. M. Breunig, C. V. Preble, A. J.
- 37 Satchwell, L. Jin, N. J. Brown, T. W. Kirchstetter and C. D. Scown, Life-Cycle Greenhouse Gas
- Emissions and Human Health Trade-Offs of Organic Waste Management Strategies, *Environ. Sci. Technol.*, 2020, **54**, 9200–9209.
- 58 S. L. Nordahl, N. R. Baral, B. A. Helms and C. D. Scown, Complementary roles for mechanical and solvent-based recycling in low-carbon, circular polypropylene, *Proceedings of the National Academy of Sciences*, 2023, **120**, e2306902120.
- 59 M. Puettmann, A. Sinha and I. Ganguly, Life Cycle Energy and Environmental Impacts of Cross Laminated Timber Made with Coastal Douglas-fir, *Journal of Green Building*, 2019, **14**, 17–33.
- 45 60K. Lan, S. S. Kelley, P. Nepal and Y. Yao, Dynamic life cycle carbon and energy analysis for cross-
- laminated timber in the Southeastern United States, *Environmental Research Letters*, 2020, **15**,
- 47 124036.

- 1 61 M. Puettmann, A. Sinha and I. Ganguly, CORRIM REPORT Life Cycle Assessment of Cross
- 2 Laminated Timbers Produced in Oregon, Consortium for Research on Renewable Industrial
- 3 Materials, 2017.
- 4 62 Athena Sustainable Materials Institute, *A Life Cycle Assessment of Cross-Laminated Timber Produced in Canad*, Athena Sustainable Materials Institute, 2013.
- 6 63 C. X. Chen, Environmental Assessment of the Production and End-of-Life of Cross-Laminated Timber in Western Washington.
- 8 64 Portland Cement Association, Environmental Product Declaration: Portland Cement, 2021.
- 9 65 World Buisness Council For Sustainable Development, *The Cement Sustainability Initative: Cement Industry Energy and CO2 Performance, Getting the Numbers Right*, 2016.
- 11 66 Worldsteel association, Life cycle inventory (LCI) study 2020 data release, 2021.
- 12 67 International Energy Agency, *Iron and Steel Technology Roadmap Analysis*, 2020.
- 68 G. J. Venta, *Life cycle analysis of gypsum board and associated finishing products*, ATHENATM
 Sustainable Materials Institute, Ottawa, Canada, 1997.
- 69 Georgia-Pacific Gypsum LLC, Type III environmental product declaration (EPD) for 1/2"
 DensDeck® Prime Roof Board, 2020.
- 70 Georgia-Pacific Gypsum LLC, Type III environmental product declaration (EPD) for 1/2"
 ToughRock® Mold-GuardTM Panel, 2020.
- 71 Georgia-Pacific Gypsum LLC, Type III environmental product declaration (EPD) for 1/2"
 ToughRock® Lite-Weight Panel, 2020.
- 72 Georgia-Pacific Gypsum LLC, *Type III environmental product declaration (EPD) for 1/2"*22 *ToughRock® Fireguard C® Panel*, 2020.
- 73 Georgia-Pacific Gypsum LLC, *Type III environmental product declaration (EPD) for 1/2"*24 DensArmor Plus® C Panel, 2020.
- 74F. Pierobon, M. Huang, K. Simonen and I. Ganguly, Environmental benefits of using hybrid CLT
 structure in midrise non-residential construction: An LCA based comparative case study in the U.S.
 Pacific Northwest, *Journal of Building Engineering*, 2019, 26, 100862.
- 75B. Bose, T. P. Hendrickson, S. L. Nordahl, S. Kane, J. Fan, S. A. Miller and C. D. Scown, Life-cycle carbon footprint and total production potential of cross-laminated timber from California's wildland-urban interface, *Environ. Res. Lett.*, 2025, **20**, 094046.
- 76S. Kane and S. A. Miller, Predicting biochar properties and pyrolysis life-cycle inventories with compositional modeling, *Bioresource Technology*, 2024, **399**, 130551.
- 33 77 A. Marmier, Decarbonisation Options for the Cement Industry.
- 34 78S. Kane, A. Bin Thaneya, A. P. Gursel, J. Fan, B. Bose, T. P. Hendrickson, S. L. Nordahl, C. D.
- Scown, S. A. Miller and A. Horvath, Uncertainty in determining carbon dioxide removal potential of biochar, *Environ. Res. Lett.*, DOI:10.1088/1748-9326/ad99e9.
- 37 79 S. Nikfar, A. Fahimi and E. Vahidi, Unlocking sustainable lithium: A comparative life cycle
- assessment of innovative extraction methods from brine, *Resources, Conservation and Recycling*,
 2025, 212, 107977.
- 40 80 D. N. Beatty, S. L. Williams and W. V. Srubar, Biomineralized Materials for Sustainable and Durable Construction, *Annual Review of Materials Research*, 2022, **52**, 411–439.
- 42 81 N. Alaux, H. Vašatko, D. Maierhofer, M. R. M. Saade, M. Stavric and A. Passer, Environmental
- potential of fungal insulation: a prospective life cycle assessment of mycelium-based composites, *Int J Life Cycle Assess*, 2024, **29**, 255–272.
- 45 82E. Van Roijen and S. A. Miller, Leveraging biogenic resources to achieve global plastic
- decarbonization by 2050, *Nat Commun*, 2025, **16**, 7659.

- 1 83 A. Bin Thaneya, A. P. Gursel, S. Kane, S. A. Miller and A. Horvath, Assessing uncertainty in
- building material emissions using scenario-aware Monte Carlo Simulation, *Environ. Res.: Infrastruct.* Sustain., DOI:10.1088/2634-4505/ad40ce.
- 4 84 A.-M. Iosif, F. Hanrot, J.-P. Birat and D. Ablitzer, Physicochemical modelling of the classical steelmaking route for life cycle inventory analysis, *Int J Life Cycle Assess*, 2010, **15**, 304–310.
- 85 G. Wernet, S. Hellweg, U. Fischer, S. Papadokonstantakis and K. Hungerbühler, Molecular-Structure-Based Models of Chemical Inventories using Neural Networks, *Environ. Sci. Technol.*,
- 8 2008, **42**, 6717–6722.
- 9 86 A. Habibi, O. Bamshad, A. Golzary, R. Buswell and M. Osmani, Biases in life cycle assessment of circular concrete, *Renewable and Sustainable Energy Reviews*, 2024, **192**, 114237.
- 87 M. N. Nwodo and C. J. Anumba, Exergetic Life Cycle Assessment: A Review, *Energies*, 2020, **13**, 2684.
- 13 88 J. Dewulf, M. E. Bösch, B. De Meester, G. Van der Vorst, H. Van Langenhove, S. Hellweg and M. a.
- J. Huijbregts, Cumulative exergy extraction from the natural environment (CEENE): a
- 15 comprehensive life cycle impact assessment method for resource accounting, *Environ Sci Technol*, 2007, **41**, 8477–8483.
- 89 L. Wang, C. Violet, R. M. DuChanois and M. Elimelech, Derivation of the Theoretical Minimum Energy of Separation of Desalination Processes, *J. Chem. Educ.*, 2020, **97**, 4361–4369.
- 90 R. Song, A. A. Keller and S. Suh, Rapid Life-Cycle Impact Screening Using Artificial Neural Networks, *Environ. Sci. Technol.*, 2017, **51**, 10777–10785.
- 91 A. Martínez, J. Fan and S. A. Miller, Machine learning in life cycle assessment and low carbon material discovery: Challenges and pathways forward for the construction industry, *Resources*, *Conservation and Recycling*, 2026, **224**, 108567.
- 24 92 C40 Knowledge Hub, 2024.

- 93 Praneet Arshi and Kendal Smith, Harvesting hardware: Our approach to carbon-aware fleet
 deployment, Google, 2025.
- 27 94 City of Vancouver, Embodied Carbon Guidelines, 2023.
- 95 A. Hasanbeigi, D. Shi and N. Bhadbhade, Federal Buy Clean for Cement and Steel Policy Design
 and Impact on Industrial Emissions and Competitiveness, Global Efficiency Intelligence, 2021.
- 30 96 Marin County, Carbon Concrete Requirements, 2025.
- 31 97 European Comission, Carbon Border Adjustment Mechanism, .

Supplemental Information:

A framework for ground-up life cycle assessment of novel, carbon-storing building materials

Seth Kane ^{a, †}, Baishakhi Bose ^b, Thomas P. Hendrickson ^c, Jin Fan ^a, Sarah L. Nordahl ^c, Corinne D. Scown ^{b,c,d,e}, Sabbie A. Miller ^a

^a Department of Civil and Environmental Engineering, University of California, Davis
^b Biological Systems and Engineering Division, Lawrence Berkeley National Laboratory
^c Energy Analysis and Environmental Impacts Division, Lawrence Berkeley National Laboratory

^d Joint BioEnergy Institute, Lawrence Berkeley National Lab

^e Energy & Biosciences Institute, University of California, Berkeley

† Corresponding Author: T +1 907 750 6364, E skane@ucdavis.edu

1. Supplemental Introduction

In addition to the description of ordinary Portland cement and yellow poplar cross-laminated timber presented in the main text, additional mineral and biogenic materials were examined with the developed framework to provide additional examples of its application. For mineral-derived materials, these additional examples included the production of low-carbon steel and gypsum board. These materials represent the 2nd and 3rd most consumed, chemically processed mineral-derived materials in the US, and combined with cement, are responsible for 64% of total US chemically processed industrial minerals production. In addition, they provide insight into applying this framework to meaningfully different processes than cement production and how this framework can provide increased insight into critical LCA decision-making for the treatment of drying, co-products, waste resources, feedstocks, and industrial symbiosis. We also provide additional modeling details for biogenic resources, including example composition and carbon uptake data, and emission factors used for the analysis in the main text. While key results for these materials are given in the main text, here we provide complete model and process descriptions, as well as additional results.

2. Supplemental Methods

2.1 Biogenic material phases

Supplemental Table 1. Biomolecular composition across ten compounds for example biomass materials.

	Acetate	Ash	Cellulose	Hemicellulose	Lignin	Proteins	Butyric Acid	Extractive	Source
Sorghum	2.20%	4.00%	30.00%	20.70%	21.00%	4.39%	0.00%	17.71%	[4]
Corn stover	2.20%	5.77%	35.50%	25.31%	16.24%	3.70%	0.00%	11.28%	[5,6]
Miscanthus	0.50%	2.79%	41.42%	25.76%	21.41%	0.40%	7.72%	0.00%	[5,7]
Switchgrass	2.46%	3.45%	34.21%	21.54%	19.60%	4.88%	0.00%	13.86%	[4]
Pine	0.00%	0.07%	29.82%	13.48%	24.74%	0.00%	0.00%	31.89%	[8]
Walnut	0.00%	19.23%	26.29%	9.92%	17.63%	0.00%	0.00%	26.93%	[8]
Almond	0.00%	8.13%	38.54%	16.06%	21.63%	0.00%	0.00%	15.64%	[8]
Fir	0.00%	0.08%	28.46%	12.02%	23.42%	0.00%	0.00%	36.02%	[8]
Yellow Poplar			39.3%	18.4%	21.4%				[9]
Kraft Lignin (Eucalyptus)			1.7%	1.8%	98.2%				[10]
Kraft Lignin (Poplar)			1.3%	4.3%	91.0%				[10]
Kraft Lignin (Olive tree residue)			12.2%	10.3%	72.0%				[10]

Supplemental Table 2. Carbon content and carbon uptake for example biomass materials.

	Carbon C	ontent (%)	Carbon (MT CC	Source	
	Low	High	Low	High	
Sorghum	41.9%	44.6%	20.9	26	[11]
Corn stover	43.7%	44.8%	1.9	13.2	[12,13]
Miscanthus	44.6%	44.7%	36.2	42.2	[14]
Switchgrass	44.0%	45.7%	24.7	34.5	[11]
Pine	46.1%	48.2%	9.3	18.2	[15,16]
Walnut	46	5%	0.1	2.2	[17,18]
Almond	45	5%	5	.9	[19,20]
Yellow Poplar	38.1%	43.5%	14.9	17.0	[21,22]
Fir	40.9%	49.1%	12.8	15.4	[23]
Lignin	60%	65%	N/A	N/A	[24]

2.1 Additional cement modeling details

Marl and cement rock calcium sources reported by the USGS as ~9% of total calcium sourcing for cement are composed primarily of calcite and kaolinite phases and, therefore, are modeled identically to these two phases in limestone and kaolin. Silica (SiO₂) from silica sand, quartzite, and sandstone is used as the only silicon source. We note that numerous secondary silica sources (fly ash, steel slag, etc.) are reported by the USGS and are not included in this assessment. Both gibbsite (Al(OH)₃) and kaolinite (Al₂O₃ 2SiO₂·2H₂O) are examined as aluminum sources. Kaolinite is obtained from kaolin clay (57.4% of aluminum) and shale (31.1% of aluminum). Gibbsite is examined from bauxite aluminum ores (11.4% of aluminum). Other aluminum-containing mineral phases in bauxite are not included in this analysis. The hematite (Fe₂O₃) phase in iron ore is modeled as the iron source. Other iron-containing phases were excluded.

Supplemental Table 3. Formation reactions of cement phases.

Cement phase	Wt. fraction	Raw mineral phase	Reaction	Phase production fraction
Alite	63%	Calcite, silica	$3\text{CaCO}_3 + \text{SiO}_2 \rightarrow \text{Ca}_3 \text{SiO}_5 + 3\text{CO}_2$	100%
Belite	15%	Calcite, silica	$2CaCO_3+SiO_2 \rightarrow Ca_2SiO_4+2CO_2$	100%
Aluminat e	9%	Calcite, gibbsite	$3CaCO_3+2Al(OH)_3 \rightarrow Ca_3Al_2O_6+3CO_2+3H_2O$	12.9%
		Calcite, kaolinite	$3CaCO_3+Al_2Si_2O_5(OH)_4 \rightarrow Ca_3Al_2O_6+3CO_2+2SiO_2+2H_2O$	87.1%
Ferrite	8%	Calcite, gibbsite, hematite $4CaCO_3+2Al(OH)_3+Fe_2O_3 \rightarrow Ca_4Al_2Fe_2O_{10}+4CO_2+3H_2O_{10}$		12.9%
		Calcite, kaolinite, hematite	$4\text{CaCO}_3 + \text{Al}_2\text{Si}_2\text{O}_5(\text{OH})_4 + \text{Fe}_2\text{O}_3 \rightarrow \text{Ca}_4\text{Al}_2\text{Fe}_2\text{O}_{10} + 4\text{CO}_2 + 2\text{H}_2\text{O} + 2\text{SiO}_2$	87.1%
		Gypsum Used as mined.		65.5%
Gypsum	5%	Calcite	$CaCO3 \rightarrow CaO + CO2;$ $CaO+SO_2+2H_2O+0.5O_2 \rightarrow (CaSO_4\cdot 2H_2O)$	34.5%

As mining LCI data included some crushing at the mine, an 80% passing particle size (*F*) for Bond's equation of 50,800 μm was used for all resources except silica sand (2,000 μm) and clay (2 μm). Ending 80% passing particle sizes (*P*) of 10 μm for all materials except clay (2 μm). For post-pyroprocessing milling, a starting size of 25,000 μm was used, and an ending size of 10 μm was used. Bond's Index values of 45.6 kJ/kg for limestone, 85.7 kJ/kg for silica sand, 28.6 kJ/kg for clay, 38.0 kJ/kg for Bauxite, 46.6 kJ/kg for iron ore, 26.2 kJ/kg for gypsum, and 51.9 kJ/kg for cement clinker were used.²

2.1 Steel process description

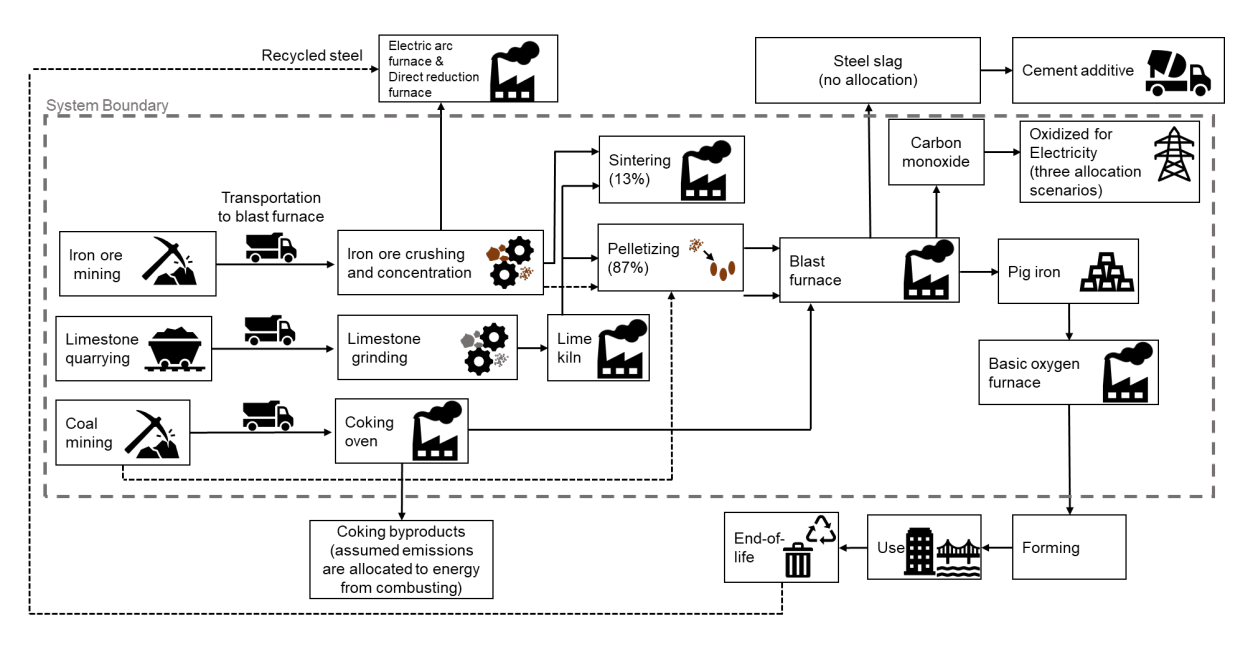
2.1.1 Scope

Low-carbon steel production is modeled as the average US primary production of direct-shipped iron ore, which requires no chemical benefaction prior to sintering or pelletization.³ A blast furnace-basic oxygen furnace system is examined, as this is the predominant method of primary steel production in the US, comprising 96.5% of total domestic primary steel production as of 2019.⁴ The herein-used system boundary used to produce steel is shown in Supplemental Figure 1. The system is examined with a functional unit of 1 kg steel billet.

In the primary analysis, no allocation of emissions to the steel slag co-product is performed. In comparison with Worldsteel⁵ and International Energy Agency (IEA)⁶ steel emission values, we apply a system expansion approach to account for slag replacement of primary cement

production, using the emissions and energy for cement production as calculated in the main text. No allocation is performed to coking co-products – all emissions associated with potential downstream processing or use of these products are excluded. Three allocation scenarios are considered for energy produced from the combustion of blast furnace and basic oxygen furnace gas: (1) all emissions allocated to steel, (2) system expansion replacing primary electricity production (consistent with EIA modeling), and (3) all emissions allocated to energy.

Emissions associated with transportation are omitted, but past assessments have estimated energy use for transportation as 0.03 MJ/kg steel,⁵ or 0.2% of the herein calculated energy use. We do not assign emissions associated with the upstream processing of fuels, with the exception of stoichiometrically required metallurgical coke.



Supplemental Figure 1. System boundary to produce low-carbon steel.

2.1.2 Material composition and preparation

Iron ore composition is modeled as 63.72% Fe, 3.41% SiO₂, and 2.42% Al₂O₃, with iron present as 80% Fe₂O₃ (hematite) and 20% Fe₃O₄ (magnetite). All moisture present in ores or added during benefaction is assumed to be dried with waste heat. Prior to thermal processing, iron ore particle size is modeled as crushed at the mine to 50.8 mm and ground/milled to 2.59 mm for sintering and 50 μ m for pelletizing. Energy inputs for crushing are accounted for in the mining inventories and grinding energy requirements are described with Bond's equation (see the main text). Other particle sizes before and after milling are bituminous coal for pelletizing 50.8 mm to 50 μ m, anthracite coal for coking 50.8 mm to 25.4 mm, and limestone 50.8 mm to 125 μ m, with the Bond's Index values described by Bond and in more recent studies. 2.8

2.1.3 Pelletizing, sintering, coking, and calcination reactions

Prior to the blast furnace, 13% of ore is sintered, while 87% is pelletized.⁴ Sintering is modeled with the following reactions:

$$CaO+SiO_2 \rightarrow CaSiO_3$$

 $3Fe_2O_3 \rightarrow 2Fe_3O_4 + 0.5 O_2$

26 wt.% of SiO₂ present in the iron ore (0.89 wt.% of total ore) is assumed to form CaSiO₃ during sintering,⁹ and 1.7 mol CaO is added per mol SiO₂ reacted during sintering.³ Sinter iron composition is modeled as 93 wt.% Fe₃O₄ and 7 wt.% Fe₂O₃. An energy efficiency of 26% is used for sintering,¹⁰ with an energy source of coke.

Pellets are modeled with a composition of 98 wt.% iron ore, 1 wt.% CaCO₃, and 1 wt.% anthracitic coal. Pelletizing energy requirements are met with the included anthracitic coal (emission factor of 0.0982 kg CO₂/MJ¹¹), with the remainder being met with blast furnace gas (emission factor of 0.26 kg CO₂/MJ¹¹). Due to limited chemical reactions during pelletizing, the energy consumption during pelletizing is modeled directly as 0.5 MJ/kg steel, ¹² excluding the energy produced by the combustion of coal inherent in pellets. This energy is primarily consumed for heating and phase transitions.

Pyrolysis of bituminous coal to form metallurgical coke is modeled based on previous experimentally determined enthalpies ($\Delta H_{Rxn} = 0.02651$ MJ/kg) and reactions (CO₂ emissions of 0.08586 kg/kg, and H₂O emissions of 0.860 kg/kg).^{1,13} Coke yields are modeled as 70% of initial coal inputs, and coke is assumed 86% carbon,¹⁴ with the remainder ash. The energy efficiency of coking is modeled as 51.2%, excluding energy recovery of flue gas co-products.¹⁵ Therefore, emissions associated with the combustion of coking flue gas co-products are assumed to be allocated to energy produced by the combustion of those products and are excluded. Fuel inputs to coking ovens are modeled as a mixture of coking byproduct gas and blast furnace gas, with the composition previously reported.¹⁵ This mixed gas has a LHV of 3.161 MJ/kg and CO₂ emissions of 0.18 kg CO₂/MJ, assuming complete combustion.

Limestone is used as the lime feedstock, and is calcined to form lime (CaO), with a thermal efficiency of 54.05%, and a fuel source of natural gas.

2.1.4 Blast furnace and basic-oxygen furnace reactions

Reactions in the blast furnace are modeled based on the stoichiometric minimum carbon and oxygen content, with the assumption that pig iron is 3 wt.% C:¹

$$Fe_2O_3 + 3.279C + \rightarrow 2(Fe \cdot 0.1395C) + 3 CO$$

 $Fe_3O_4 + 4.418C \rightarrow 3(Fe \cdot 0.1395C) + 4 CO$

With the combustion of blast furnace gas to produce electricity:

$$3\text{CO}+1.5\text{O}_2 \rightarrow 3\text{CO}_2$$
 (presented per 1 mol Fe₂O₃/2 mol pig iron)
 $4\text{CO}+2\text{O}_2 \rightarrow 4\text{CO}_2$ (presented per 1 mol Fe₃O₄/3 mol pig iron)

Slagging is modeled with lime added to reach a 1.7 CaO/SiO₂ molar ratio, with the assumption that all excess CaO reacts with Fe₂O₃ to form CaFe₂O₄ with the equation:

$$Fe_2O_3+CaO \rightarrow CaFe_2O_4$$

Lime reacts with SiO₂ with the same reaction as during sintering. Alumina present in iron ore and slag is modeled as non-reactive. Other reactions, including the reaction of phosphorus, manganese, and sulfur into slag, are excluded, due to their lower and highly variable content in iron ore. All blast furnace reactions are modeled with an energy efficiency of 39.13%, ¹⁶ with a fuel source of 89% metallurgical coke, 7% electricity (at US average emission factor), and 4% natural gas. ¹⁷ The energy efficiency of the oxidation of carbon monoxide to produce electricity is modeled as 37%. ⁶

Reduction of hematite and magnetite to pig iron and carbon monoxide is endothermic (ΔH_{Rxn} = 247.25 and 225 kJ/mol pig iron for hematite and magnetite, respectively). However, when including the oxidation of carbon monoxide to carbon dioxide, the entire process is net exothermic (ΔH_{Rxn} = -177.25 and -152.333 kJ/mol pig iron for hematite and magnetite, respectively). Herein, we assign efficiency factors to both the endothermic and exothermic portions separately. Oxidation of carbon monoxide is assumed to replace primary electricity production, consistent with assumptions previously made by the IEA.⁶ Here, we examine three allocation scenarios for CO_2 emissions associated with the oxidation of carbon monoxide to the energy product: (1) all oxidation emissions allocated to low-carbon steel, (2) system expansion to include equivalent primary electricity production, and (3) all oxidation emissions allocated to electricity. We note that in Scenario 2, the emissions of steel are therefore dependent on the electricity grid and the specific location. For example, if the energy co-product of steel production were replacing a coal-heavy electric grid, steel production would be assigned lower emissions. If the energy co-product were replacing a low-carbon renewable energy grid, the emissions allocated to steel would be higher.

Basic oxygen furnaces were used to convert pig iron produced in the blast furnace to low-carbon steel, by reducing the carbon content from 3 wt.% to 0.1 wt.% with the reactions:

$$(Fe \cdot 0.1395C) + 0.067 O_2 \rightarrow (Fe \cdot 0.00465C) + 0.134CO$$

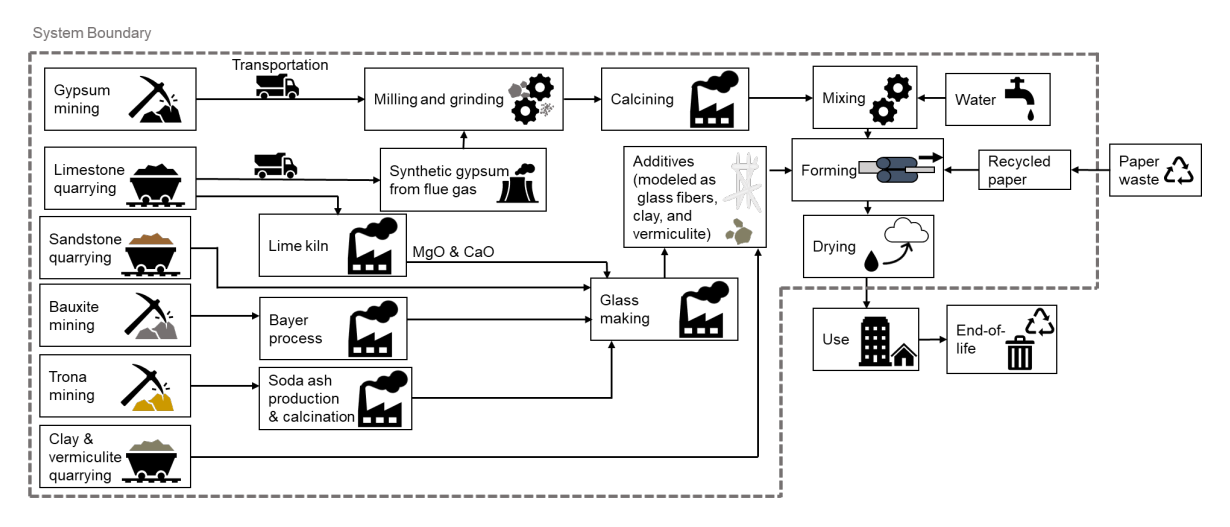
This reaction is exothermic and is assumed to follow immediately after the blast furnace, requiring no additional energy inputs. Oxidation of CO to CO₂ is modeled as described for the blast furnace, with the same allocation scenarios considered.

Facility overhead was determined based on the values reported by the MECS¹⁷ and normalized to per kg of material based on the US steel production reported by the USGS Mineral Yearbook.⁴ We note that this value also includes overhead for electric arc furnace and recycled steel production pathways, due to a lack of more granular data. This results in overhead energy consumption of 0.169 MJ/kg of low-carbon steel electricity and 0.795 MJ/kg of thermal and steam energy. We assume electricity is met at the US energy grid average emission factor, and thermal energy is met with the steel industry average of fuel resources, as reported by MECS.

2.2 Gypsum board process description

2.2.1 Scope

Production of gypsum board is modeled herein as regular type, 1/2 inch thickness, as this is the most produced gypsum board type in the US, at 95% of regular type production and 50% of all gypsum board production.⁴ Other thicknesses of regular gypsum board (5/8 inch) or types (e.g., type X) gypsum board are excluded from this analysis.¹⁸ The process flows and the system boundary used for the LCI of the regular gypsum board shown in Supplemental Figure 2. Paper in the gypsum board manufacturing process was modeled as recycled paper and was modeled with the same approach as mineral resources, as the chemical reaction approach can be applied to model the recycling process. The framework could be adapted to also apply the biogenic approach if primary paper was produced for use in gypsum board or could be extended to other types of gypsum board. A functional unit of 1 kg of gypsum board was used.



Supplemental Figure 2. System boundary and process flow diagram to produce gypsum board.

2.2.2 Gypsum board composition

Gypsum board typically contains mined gypsum (CaSO₄·2H₂O), synthetic gypsum (CaSO₄·2H₂O), vermiculite, clay, glass, and paper.¹⁹ The ratio of these mineral phases may vary depending on the type and thickness of gypsum board but is modeled herein with ratios typical of a regular type (1/2 inch) of gypsum board (89% gypsum, 5% paper, 2% vermiculite, 2% clay, 2% glass).²⁰ A ratio of 65.5% mined gypsum to 34.5% synthetic gypsum is used, based on ratios of total US gypsum consumption.⁴ The compositions of glass fibers were modeled based on a composition of 70% silica, 15% sodium oxide, 10% lime, 5% magnesium oxide, and 1% alumina.

2.2.3 Gypsum board formation

The formation of each phase in gypsum board was modeled with calcination and sulphuration reactions to form synthetic gypsum and calcining reactions prior to gypsum mixing and forming (Table 1). Vermiculite and clay were modeled as being used as quarried, and paper was modeled as recycled, which comprises ~100% of US gypsum board production. Glass production was modeled with previously described formation reactions. Glass

The intermediate calcination of gypsum is modeled to account for the consumption of water and energy, with the assumption that neither heat nor water is recycled. The process involving mined gypsum is represented in two distinct reaction steps. The first step, as detailed in Table 1, involves the emission of H₂O; typically, this chemically-derived water is not recycled. Therefore, the water and energy consumption are modeled in the second reaction step of the gypsum synthesis process. Similarly, the process of using synthetic gypsum to produce gypsum board involves four steps. First, lime is produced from calcite and used in flue gas desulphurisation (FGD), as shown in Table 1. The following two steps of producing gypsum board from synthetic gypsum are modeled as the same as the mined gypsum process. The water and energy consumption are modeled in the second and third steps.

Supplemental Table 4. Formation reactions of gypsum board phases.

Gypsum board phase	Weight fraction	Raw mineral phase	Reaction	Phase production fraction	
Gypsum	89%	Gypsum (mined)	$CaSO_4 \cdot 2H_2O \rightarrow$ $(CaSO_4 \cdot 0.5H_2O) + 1.5H_2O$	65.5%	
		Calcite (synthetic gypsum)	$CaCO3 \rightarrow CaO + CO_2;$	34.5%	
			$CaO+SO_2+2H_2O+0.5O_2 \rightarrow (CaSO_4\cdot 2H_2O)$		
		Gypsum anhydrite	$(CaSO_4 \cdot 0.5H_2O) + 1.5H_2O \rightarrow$ $CaSO_4 \cdot 2H_2O$	100%	
Paper	5%	Paper	Used as recycled	100.0%	
Vermiculite	2%	Vermiculite	No chemical processing	100.0%	
Clay	2%	Clay	No chemical processing	100.0%	
Glass	2%	Trona	US LCI data used.	100%	

2.2.4 Processing of raw materials for gypsum board

Mineral composition was determined based on previously reported mineralogy of limestone, silica sand, bauxite, salt rock, trona, magnesite, and gypsum resources. Many of the resources used in the production of gypsum board are high purity, such as limestone at 98% calcite,²¹ silica sand at 99% silica,²² and gypsum at 92% gypsum.²³ In contrast, trona (82.4% sodium carbonate)²⁴ and bauxite (53.17% gibbsite)²⁵ are typically less pure and therefore require more raw material relative to their stoichiometric requirement. Impurities in paper recycling were not considered, and both clay and vermiculite are typically used as mined. LCIs for all mining processes are from the US Lifecycle inventory database.²⁶

2.2.5 Material manufacture and assembly for gypsum board

The pyroprocessing efficiency is assumed to be 35.3% based on previous data from case studies.^{27,28} Glass fiber CO₂ emissions and energy use were determined from US LCI data.²⁹ The energy used in both gypsum calcining and post-forming drying is assumed to be met with natural gas. Lime production as a feedstock for synthetic gypsum production is modeled as 41.89% thermally efficient, with natural gas as the fuel source.

Material losses due to dust, spillage, and other sources were modeled with the same assumptions as in the Portland cement example for the mining (3%), milling and grinding (3%), pyroprocessing (3%), post-processing (3%), storage (1%), and transportation (3%) steps of the production process. As losses are applied multiplicatively, material losses downstream of the pyroprocessing step result in a net increase in mass flow through the high-emission and energy-requiring pyroprocessing step by 7.15%.

The transportation distances between gypsum quarries and gypsum board production facilities are often considered negligible,³⁰ as facilities are located near gypsum quarries, and relatively small amounts of other minerals are used. Similarly, the transport distances for synthetic gypsum production from quarries to flue-gas desulfurization locations have been considered negligible.³⁰ Facility overhead values of HVAC (0.01 MJ/kg gypsum board) and facility lighting (0.01 MJ/kg gypsum board) are assumed to be the same as those of Portland cement, due to a lack of reported data. Overhead energy consumption for packing and storage (0.04 MJ/kg gypsum board) and onsite transportation (0.03 MJ/kg gypsum board) are used based on previously reported energy consumption.²⁷

2.3 Additional methodology for biogenic materials

Supplemental Table 5: Life cycle inventory inputs for each stage of processing to produce 1 m³ of CLT.

Processing Stage	Input Parameter	Unit	YP	ЕН	Notes
	Equipment	kg	0.36*	0.33*	*include both use and maintenance
Harvesting	Gasoline	MJ	24	19	
Operations	Diesel	MJ	175	151	
	Lubricant	kg	0.3	0.2	
	Coal	MJ	_	734	
	Natural Gas	MJ	602	181	
Sawmill	Gasoline	MJ	20.0	_	
Operations	Diesel	MJ	198	_	
орегиноны	Oil	MJ	0.7	268.5	
	Wood	MJ	1069.4*	3899*	*residues from sawmill operations
	Resin	kg	5.9	5.5	
CLT Mill	Electricity	kWh	118	111	
	Natural Gas	MJ	92	86	
Transportation to	Flat Bed Truck	km	50	50	
Transportation to Sawmill	Logs Transported	mt	0.87	0.81	
Transportation to	Flat Bed Truck	km	61.2	61.2	
CLT Mill	Logs Transported	mt	0.52	0.48	

Supplemental Table 6: Life-cycle GHG intensities for the life cycle inventory inputs used in this study.

		Life-	References			
Parameter	CH ₄	NO ₂	CO ₂	CO ₂ e	Unit [†]	
Equipment				46.6	kg/dry ton wood	31
Gasoline*	1.4E-04	8.0E-07	1.0E-01		kg/MJ	Upstream emissions calculated
Coal*	1.6E-04	1.5E-06	9.4E-02		kg/MJ	using AgileC2G and data from Nordahl <i>et al.</i> 2023. ³²
Oil*	9.2E-05	6.2E-07	7.7E-02		kg/MJ	Combustion emissions are calculated using data from the US EPA. ³³
Natural Gas*	1.1E-04	3.3E-08	5.9E-02		kg/MJ	Upstream and combustion emissions calculated using
Diesel*	1.1E-04	1.1E-06	9.3E-02	1	kg/MJ	AgileC2G and data from Nordahl <i>et al.</i> 2023. ³²
Lubricant	4.9E-04	2.7E-06	1.9E-01		kg/kg	31
Wood	9.6E-03	4.2E-03			kg/kg	34
Resin	2.1E-03	1.8E-04	5.6E-01		kg/kg	31
Electricity	1.4E-05	2.1E-04	2.3E-01		kg/KWh	33
Flat Bed Truck	2.7E-04	6.4E-07	2.1E-01		kg/Mt-km	31

^{*}Includes both upstream emissions and combustion emissions.

3. Supplemental Results

Material composition was determined based on previously reported mineralogy of limestone, silica sand, bauxite, clay, ferrous ore, and gypsum resources. Many of the resources used in the production of Portland cement are high purity, such as limestone at 98% calcite²¹, silica sand at 99% silica²², and gypsum at 92% gypsum.²³ In contrast, bauxite (53.17% gibbsite²⁵), clay (41% kaolinite³⁵), and ferrous ore (64% hematite³⁶) are typically less pure and therefore require more raw material relative to their stoichiometric requirement (Main text Figure 5a). We note that we do not account for impurities that could replace other primary resources. For example, reasonable quantities of silica are present in both clay (8%) and bauxite (6.3%). Unaccounted-for impurities may increase energy consumption associated with mining, grinding, and milling processing steps, but given the high uncertainty and spatial variability in mineral composition, not accounting for these impurities provides a conservative estimate for the energy requirement of these processes.

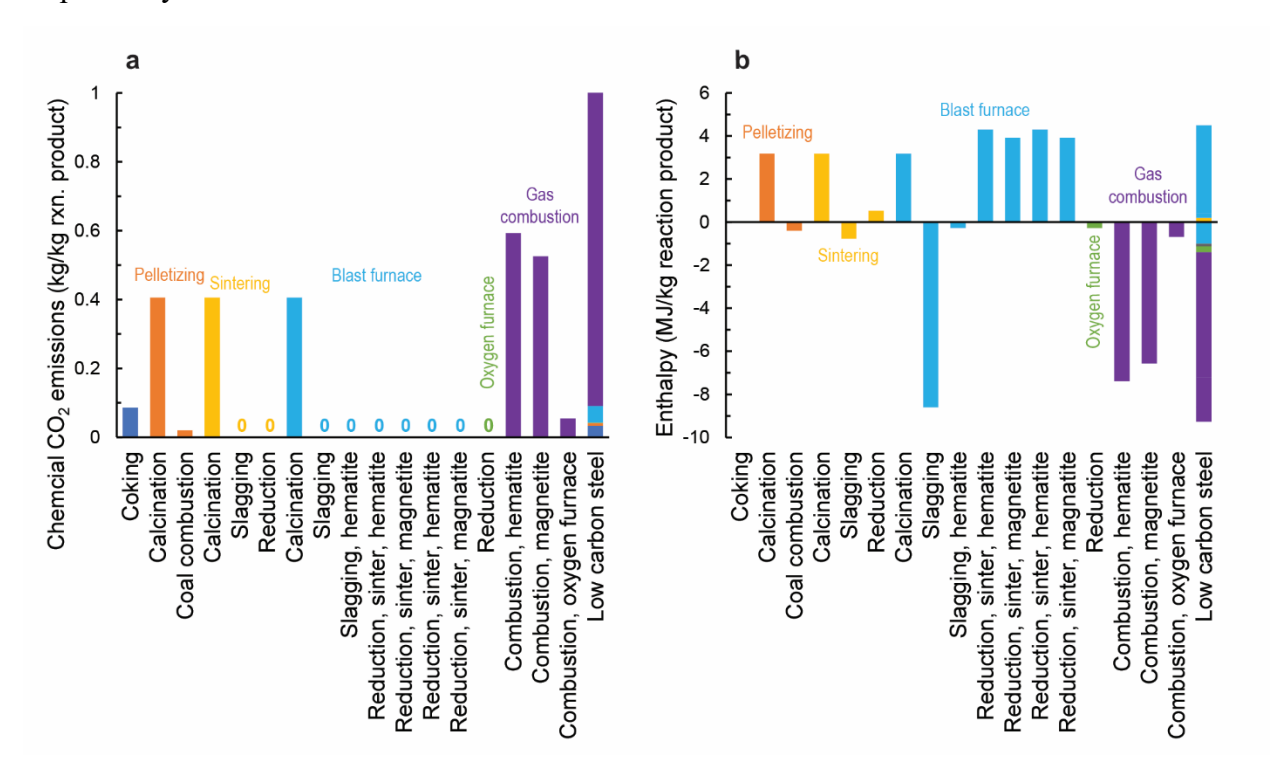
3.1 Steelmaking

Mineral feedstocks in steelmaking are dominated by inputs of ferrous ore (1.555 kg/kg steel), and bituminous coal for coking (0.581 kg/kg steel), in addition to a small portion of limestone (0.129 kg/kg steel, Supplemental Figure 3). In total, 2.25 kg of mineral inputs are required to produce 1 kg of steel, excluding material waste during processing. When including material

waste after the mine, an additional 0.28 kg of minerals are consumed, resulting in 2.53 kg total mineral resource consumption per kg of steel.

When comparing the three allocation scenarios, the allocation of all furnace gas emissions to electricity reduces the GHG emissions of steel by 45% compared to allocating all emissions to steel. The scenario where system expansion to include US grid average electricity production is used to account for the additional energy production results in a reduction of 11.6% relative to all emissions allocated to steel. As energy consumed and produced were accounted for separately, no changes in energy consumption occurred in any allocation scenarios.

Similarly, the endothermic enthalpy requirement of steelmaking is predominantly driven by the blast furnace processing step, at 78% of the total of 4.5 MJ/kg steel required enthalpy. Exothermic reactions, primarily due to combustion of blast furnace and oxygen furnace gas release 9.3 MJ/kg steel enthalpy. Due to their small mass contributions, endothermic enthalpy contributions of calcination reactions and exothermic contributions of slagging reactions are relatively small, comprising 5% and 12% of the total endothermic and exothermic enthalpy, respectively.

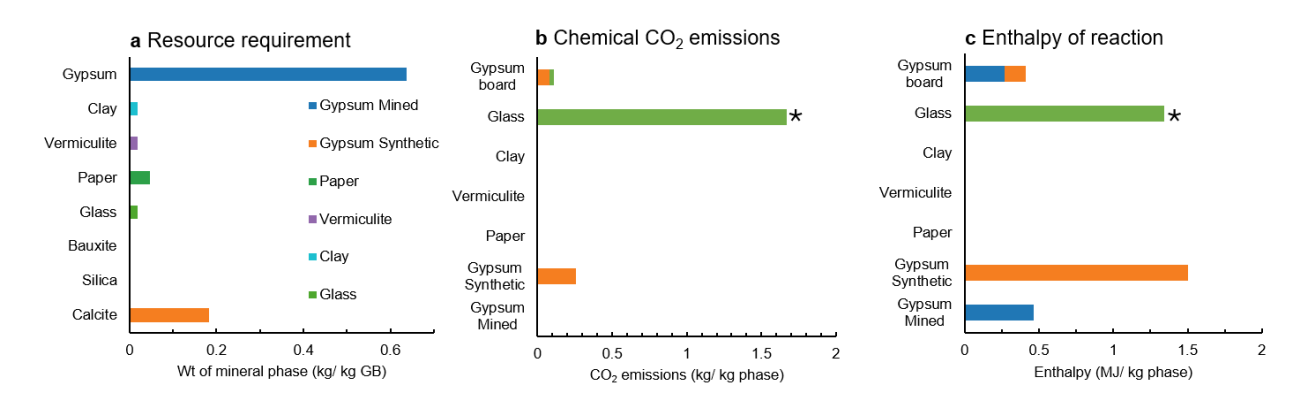


Supplemental Figure 3. (a) Chemically-derived CO₂ emissions and (b) enthalpy of reaction for steel-making reactions. Values are shown for 1 kg of reaction primary product, except the totaled low-carbon steel, which is a summation for 1 kg of low-carbon steel. No allocation of energy products from the combustion of blast or oxygen furnaces was performed at this stage of calculations.

When all emissions are allocated to steel, steelmaking emits 2.854 kg CO₂ / kg steel, driven largely by chemical emissions from the combustion of blast furnace and oxygen furnace gas.

Energy emissions due to blast furnace enthalpy and inefficiency energy consumption make up the majority of remaining emissions, and combined, these three categories comprise 85% of total CO₂ emissions. We note that these categories an area where data used in this assessment has a higher degree of certainty; blast furnace processing, efficiency data, and conversion of blast furnace gas to energy all have broadly reported and high-quality underlying data. In contrast, other processing, such as pelletizing and sintering, show higher variation between sources for underlying data such as process efficiency, and mining may have variations due to ore type. However, as these processes make up small fractions of the total CO₂ emissions, the result is relatively insensitive to variations in emissions associated with these processes. Compared to Portland cement, overhead energy consumption used for factors such as facility HVAC, lighting, and onsite transportation makes up a relatively high fraction of both emissions and energy consumption, at 7.1% of energy consumption and 3.4% of CO₂ emissions when all emissions are allocated to steel.

3.2 Gypsum board production



Supplemental Figure 4. First-principle values for the chemical conversion of raw resources into cement, including: (a) mineral mass input requirement for 1 kg gypsum board, (b) chemically-derived CO₂ emissions, and (c) energy required by the enthalpy of reaction. Results in (b) and (c) are displayed for 1 kg of each material constituent. *Glass enthalpy and chemical CO₂ emissions are shown for reference; existing LCI data are used for glass fibers.

Production of 1 mol synthetic gypsum, one of the primary mineral phases in gypsum board, results in 1 mol CO_2 for a mass ratio of 0.26 kg CO_2 / kg synthetic gypsum. However, as gypsum production relies heavily on natural gypsum, which has no associated chemically-derived emissions, the total resulting chemically-derived emissions for gypsum board is 0.084 kg CO_2 / kg gypsum board. Notably, however, production of synthetic gypsum also sequesters 1 mol of SO_2 per mol of synthetic gypsum produced, typically from coal flues or metallurgical roasting reactions, such as those used in copper production. Despite relatively large emissions for the glass fibers on a mass basis (1.67 kg CO_2 / kg glass fiber), they have only a minor contribution to the emissions of gypsum board (0.032 kg CO_2 / kg gypsum board), due to their low mass fraction.

Similarly, the enthalpy of reaction to produce gypsum board is 0.73 MJ / kg gypsum board, due to the dehydration of gypsum (Supplemental Figure 4c) as it has both notable enthalpy of formation and it is the phase present in the greatest quantity. Per kg of each phase, glass has the largest contribution to the required enthalpy of formation for gypsum board at 1.34 MJ / kg glass. We note that the exothermic enthalpy of reaction of synthetic gypsum was treated as zero, assuming that the heat in this process was not reused. However, the framework could be adapted to a case where heat present in flue gas is used, and appropriate allocation applied as in the low-carbon steel example.

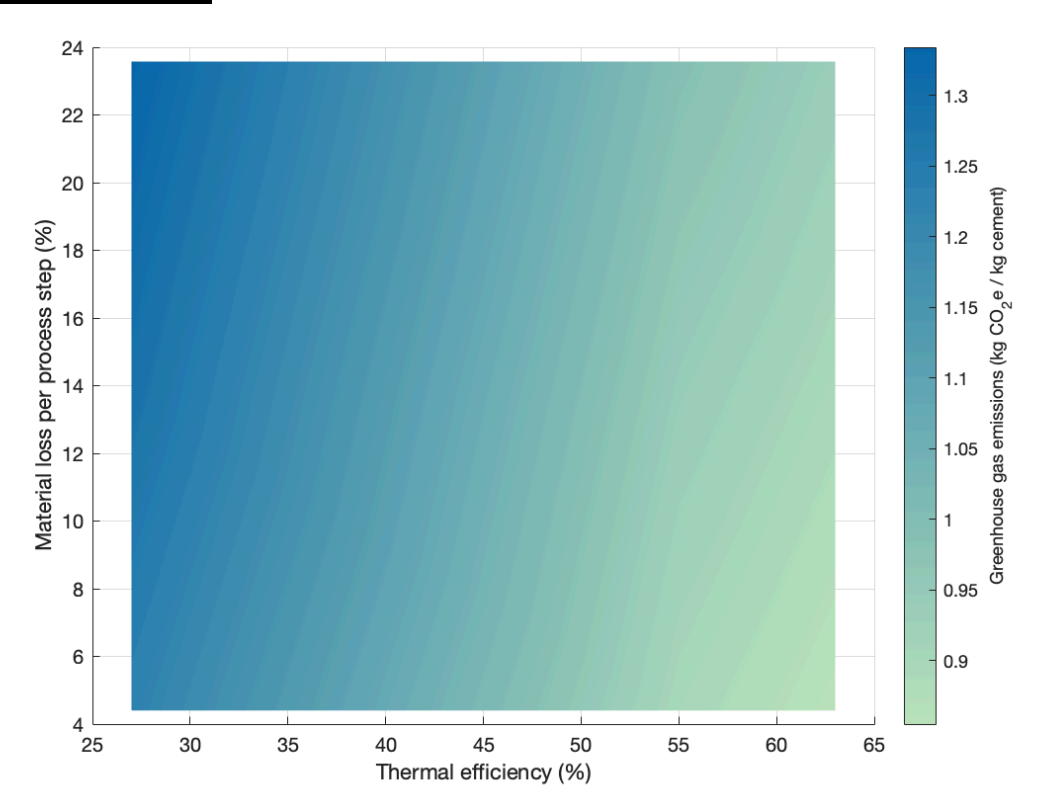
As a result of mineral impurities and mass loss due to material waste and chemically derived emissions, a total mass of 0.94 kg raw material is required per kg gypsum board, exclusive of water (Main text Figure 7b). The extracted mineral is smaller than 1 kg because the production of synthetic gypsum involves a reaction with gas phase SO₂, which is not accounted for in the raw material requirement. Extraction of these resources consumes 1.37 MJ / kg gypsum board, with this energy being primarily natural gas, electricity, and diesel consumption in paper recycling (0.82 MJ / kg gypsum board). Grinding and milling processes of gypsum prior to calcination result in an energy consumption of 0.03 MJ / kg gypsum board. After adding excessive water in the post-milling process to make gypsum mixture, the re-drying consumed significant energy of 1.82 MJ/kg gypsum board. It is worth noting that this additional step of adding water beyond the chemical requirement to reduce viscosity prior to forming, and then evaporation of this water in the manufacturing process is associated with significant energy consumption and CO₂ emissions. Water consumption shown in Main Text Figure 7b only accounts for the chemically required water to produce gypsum powder, which did not include the excessive water added at the gypsum board manufacturing stage.

In contrast to the Portland cement and low-carbon steel examples, the energy consumption of gypsum board production is dominated by the post-processing, which consumes 33% of the total energy (Main Text Figure 8b). The post-processing energy consumption is primarily for redrying the gypsum mixture to remove excessive water that was introduced during mixing steps. Paper recycling in the raw material extraction stage plays the next largest role in energy consumption, at 60% of raw material extraction energy consumption, and 15% of total energy consumption, respectively. CO₂ emissions from the production of gypsum board are dominated by mineral extraction (25%) and followed by post-processing (23%). The total CO₂ emissions resulted from material extraction were primarily driven by the energy intensity of paper recycling. With 19% of total CO₂ emissions resulting from chemically-derived emissions from chemical conversion, primarily due to the production of synthetic gypsum. About 3% of total CO₂ emissions result from energy consumption for the pre-milling and grinding of mineral resources.

The total energy consumed to produce 1 kg of gypsum board was modeled as 5.46 MJ, which is in the range of previously reported energy use of 3.44-6.74 MJ/kg gypsum board. 18,20,37-40 Transportation of raw materials contributes to ~5% of total emissions, 30 which were excluded in this study. In addition, the variation of kiln efficiency, paper recycling technologies, and the use of excess water that needs to be evaporated could also cause the discrepancy. The GHG emissions determined herein are in good agreement with other analyses of the gypsum board industry. For example, GHGs reported in several 1/2 inch gypsum boards are in a range of 0.30-

 0.48 kg CO_2 -eq / kg gypsum board, $^{18,20,37-40}$ which shows good agreement with our proposed method of 0.44 kg CO_2 -eq / kg gypsum board.

3.3 Sensitivity Analysis



Supplemental Figure 5. Sensitivity analysis of cement production, modifying the variables with higher uncertainty and variation. Ranges shown for material loss are: 1% for each process step except storage at 0.33%, for 4.4% material loss across the entire production, to 5% for each process step, except storage at 1.67% for 23.6% for the whole process, and for thermal efficiency: 26.5%, representative of a wet kiln 63%, representative of a highly efficient dry kiln with preheater and pre-calciner.

Supplemental References

- (1) Kane, S.; Miller, S. A. Mass, Enthalpy, and Chemical-Derived Emission Flows in Mineral Processing. *J. Ind. Ecol. n/a* (n/a). https://doi.org/10.1111/jiec.13476.
- (2) Bond, F. C. Crushing & Grinding Calculations Part 1. Br. Chem. Eng. 1961, 6, 378–385.
- (3) Ullmann's Encyclopedia of Industrial Chemistry. *Ullmanns Encycl. Ind. Chem.* **2000**. https://doi.org/10.1002/14356007.
- (4) United States Geological Survey. Minerals Yearbook Metals and Minerals, 2019.
- (5) Worldsteel association. *Life Cycle Inventory (LCI) Study 2020 Data Release*; 2021. https://worldsteel.org/wp-content/uploads/Life-cycle-inventory-LCI-study-2020-data-release.pdf.
- (6) International Energy Agency. *Iron and Steel Technology Roadmap Analysis*; 2020. https://www.iea.org/reports/iron-and-steel-technology-roadmap (accessed 2024-06-20).

- (7) Umadevi, T.; Sampath Kumar, M. G.; Mahapatra, P. C.; Mohan Babu, T.; Ranjan, M. Recycling of Steel Plant Mill Scale via Iron Ore Pelletisation Process. *Ironmak. Steelmak.* **2009**, *36* (6), 409–415. https://doi.org/10.1179/174328108X393795.
- (8) de Bakker, J. Energy Use of Fine Grinding in Mineral Processing. *Metall. Mater. Trans. E* **2014**, *I* (1), 8–19. https://doi.org/10.1007/s40553-013-0001-6.
- (9) Iosif, A.-M.; Hanrot, F.; Ablitzer, D. Process Integrated Modelling for Steelmaking Life Cycle Inventory Analysis. *Environ. Impact Assess. Rev.* **2008**, *28* (7), 429–438. https://doi.org/10.1016/j.eiar.2007.10.003.
- (10) Azevedo, J. M. C.; CabreraSerrenho, A.; Allwood, J. M. Energy and Material Efficiency of Steel Powder Metallurgy. *Powder Technol.* **2018**, *328*, 329–336. https://doi.org/10.1016/j.powtec.2018.01.009.
- (11) U.S. Environmental Protection Agency. Greenhouse Gas Inventory Guidance Direct Emissions from Stationary Combustion Sources; 2016. https://www.epa.gov/sites/default/files/2016-03/documents/stationaryemissions 3 2016.pdf.
- (12) Lv, W.; Sun, Z.; Su, Z. Life Cycle Energy Consumption and Greenhouse Gas Emissions of Iron Pelletizing Process in China, a Case Study. *J. Clean. Prod.* **2019**, *233*, 1314–1321. https://doi.org/10.1016/j.jclepro.2019.06.180.
- (13) Jacob, K. T.; Seetharaman, S. Thermodynamic Stability of Metallurgical Coke Relative to Graphite. *Metall. Mater. Trans. B* 1994 251 **1994**, 25 (1), 149–151. https://doi.org/10.1007/BF02663188.
- (14) Schobert, H.; Schobert, N. Comparative Carbon Footprints of Metallurgical Coke and Anthracite for Blast Furnace and Electric Arc Furnace Use. Archival Report Prepared for Blaschak Coal Corp.
- (15) Ergul, M.; Selimli, S. An Applied Study on Energy Analysis of a Coke Oven. *Sci. Technol. Energy Transit.* **2024**, *79*, 1. https://doi.org/10.2516/stet/2023042.
- (16) Rasul, M. G.; Tanty, B. S.; Mohanty, B. Modelling and Analysis of Blast Furnace Performance for Efficient Utilization of Energy. *Appl. Therm. Eng.* **2007**, *27* (1), 78–88. https://doi.org/10.1016/j.applthermaleng.2006.04.026.
- (17) US Dept. of Energy Advanced Manufacturing Office. *Manufacturing Energy and Carbon Footprints (2018 MECS)*; 2021.
- (18) Venta, G. J. *Life Cycle Analysis of Gypsum Board and Associated Finishing Products*; ATHENATM Sustainable Materials Institute: Ottawa, Canada, 1997.
- (19) Lushnikova, N.; Dvorkin, L. 25 Sustainability of Gypsum Products as a Construction Material. In *Sustainability of Construction Materials (Second Edition)*; Khatib, J. M., Ed.; Woodhead Publishing, 2016; pp 643–681. https://doi.org/10.1016/B978-0-08-100370-1.00025-1.
- (20) Georgia-Pacific Gypsum LLC. *Type III Environmental Product Declaration (EPD) for 1/2" ToughRock® Mold-GuardTM Panel*; EPD10310; 2020.
- (21) Šiler, P.; Kolářová, I.; Bednárek, J.; Janča, M.; Musil, P.; Opravil, T. The Possibilities of Analysis of Limestone Chemical Composition. *IOP Conf. Ser. Mater. Sci. Eng.* **2018**, *379* (1), 012033. https://doi.org/10.1088/1757-899X/379/1/012033.
- (22) Vegliò, F.; Passariello, B.; Abbruzzese, C. Iron Removal Process for High-Purity Silica Sands Production by Oxalic Acid Leaching. *Ind. Eng. Chem. Res.* **1999**, *38* (11), 4443–4448. https://doi.org/10.1021/ie990156b.

- (23) Karni, J.; Karni, E. Gypsum in Construction: Origin and Properties. *Mater. Struct.* **1995**, *28* (2), 92–100. https://doi.org/10.1007/BF02473176.
- (24) Wiig, S. V.; Grundy, W.; Dyni, J. R. *Trona Resources in the Green River Basin, Southwest Wyoming*; US Geological Survey, 1995.
- (25) Chen, Q.; Zeng, W. Calorimetric Determination of the Standard Enthalpies of Formation of Gibbsite, Al(OH)3(Cr), and Boehmite, AlOOH(Cr). *Geochim. Cosmochim. Acta* **1996**, *60* (1), 1–5. https://doi.org/10.1016/0016-7037(95)00378-9.
- (26) National Renewable Energy Laboratory. *U.S. Life Cycle Inventory Database*; 2012. https://www.lcacommons.gov/nrel/search.
- (27) Pedreño-Rojas, M. A.; Fořt, J.; Černý, R.; Rubio-de-Hita, P. Life Cycle Assessment of Natural and Recycled Gypsum Production in the Spanish Context. *J. Clean. Prod.* **2020**, 253, 120056. https://doi.org/10.1016/j.jclepro.2020.120056.
- (28) Suárez, S.; Roca, X.; Gasso, S. Product-Specific Life Cycle Assessment of Recycled Gypsum as a Replacement for Natural Gypsum in Ordinary Portland Cement: Application to the Spanish Context. *J. Clean. Prod.* **2016**, *117*, 150–159. https://doi.org/10.1016/j.jclepro.2016.01.044.
- (29) National Renewable Energy Laboratory. United States Life Cycle Inventory Database, 2012. https://www.lcacommons.gov/nrel/search.
- (30) Fořt, J.; Černý, R. Carbon Footprint Analysis of Calcined Gypsum Production in the Czech Republic. *J. Clean. Prod.* **2018**, *177*, 795–802. https://doi.org/10.1016/j.jclepro.2018.01.002.
- (31) Abbas, D.; Handler, R. M. Life-Cycle Assessment of Forest Harvesting and Transportation Operations in Tennessee. *J. Clean. Prod.* **2018**, *176*, 512–520. https://doi.org/10.1016/j.jclepro.2017.11.238.
- (32) Nordahl, S. L.; Baral, N. R.; Helms, B. A.; Scown, C. D. Complementary Roles for Mechanical and Solvent-Based Recycling in Low-Carbon, Circular Polypropylene. *Proc. Natl. Acad. Sci.* **2023**, *120* (46), e2306902120. https://doi.org/10.1073/pnas.2306902120.
- (33) United States Environmental Protection Agency. Emissions & Generation Resource Integrated Database (eGRID), 2023. https://www.epa.gov/egrid.
- (34) Milota, M.; Puettmann, M. E. Life-Cycle Assessment for the Cradle-to-Gate Production of Softwood Lumber in the Pacific Northwest and Southeast Regions*. *For. Prod. J.* **2017**, *67* (5–6), 331–342. https://doi.org/10.13073/FPJ-D-16-00062.
- (35) Kaufhold, S.; Hein, M.; Dohrmann, R.; Ufer, K. Quantification of the Mineralogical Composition of Clays Using FTIR Spectroscopy. *Vib. Spectrosc.* **2012**, *59*, 29–39. https://doi.org/10.1016/j.vibspec.2011.12.012.
- (36) Lu, Liming. *Iron Ore Mineralogy, Processing and Environmental Sustainability*, 2nd ed.; Elsevier, 2021.
- (37) Georgia-Pacific Gypsum LLC. *Type III Environmental Product Declaration (EPD) for 1/2" ToughRock® Fireguard C® Panel*; EPD10310; 2020.
- (38) Georgia-Pacific Gypsum LLC. *Type III Environmental Product Declaration (EPD) for 1/2" DensArmor Plus*® *C Panel*; EPD10310; 2020.
- (39) Georgia-Pacific Gypsum LLC. *Type III Environmental Product Declaration (EPD) for 1/2" ToughRock*® *Lite-Weight Panel*; EPD10310; 2020.
- (40) Georgia-Pacific Gypsum LLC. *Type III Environmental Product Declaration (EPD) for 1/2" DensDeck® Prime Roof Board*; EPD10310; 2020.